$a \neq 0$, this domain pair can be classified as a *ferroelectric domain pair*.

Similarly, the first number a in column g_μ determines the number of independent components of the tensor of optical activity that have opposite sign in domain states $\mathbf{S}_1$ and $\mathbf{S}_j$; if $a \neq 0$, the two domain states in the pair can be distinguished by optical activity. Such a domain pair can be called a *gyrotropic domain pair*. As in Table 3.4.3.1 for the ferroelectric (ferroelastic) domain pairs, we can define a *gyrotropic phase* as a ferroic phase with gyrotropic domain pairs. The corresponding phase transition to a gyrotropic phase is called a *gyrotropic phase transition* (Koňák *et al.*, 1978; Wadhawan, 2000). If it is possible to switch gyrotropic domain states by an external field, the phase is called a *ferrogyrotropic phase* (Wadhawan, 2000). Further division into full and partial subclasses is possible.

One can also define *piezoelectric (electro-optic) domain pairs*, *electrostrictive (elasto-optic) domain pairs* and corresponding phases and transitions.

As we have already stated, domain states in a domain pair $(\mathbf{S}_1, \mathbf{S}_j)$ differ in principal tensor parameters of the transition $K_{1j} \supset F_1$. These principal tensor parameters are Cartesian tensor components or their linear combinations that transform according to an irreducible representation Γ_α specifying the primary order parameter of the transition $K_{1j} \supset F_1$ (see Section 3.1.3). Owing to a special form of K_{1j} expressed by equation (3.4.3.42), this representation is a real one-dimensional irreducible representation of K_{1j}. Such a representation associates +1 with operations of F_1 and -1 with operations from the left coset $g^\star_{1j}$. This means that the principal tensor parameters are one-dimensional and have the same absolute value but opposite sign in $\mathbf{S}_1$ and $\mathbf{S}_j = g^\star_{1j}\mathbf{S}_1$. Principal tensor parameters for symmetry descents $K_{1j} \supset F_1$ and associated Γ_α's of all non-ferroelastic domain pairs can be found for property tensors of lower rank in Table 3.1.3.1 and for all tensors appearing in Table 3.4.3.5 in the software *GI★KoBo*-1 and in Kopský (2001).

These specific properties of non-ferroelastic domain pairs allow one to formulate simple rules for tensor distinction that do not use principal tensor parameters and that are applicable for property tensors of lower rank.

(i) Symmetry descents $K_{1j} \supset F_1$ of non-ferroelastic domain pairs for lower-rank property tensors lead only to the appearance of independent Cartesian morphic tensor components and not to the breaking of relations between these components. These morphic Cartesian tensor components can be found by comparing matrices of property tensors in the twinning group K_{1j} and the low-symmetry group F_1 as those components that appear in F_1 but are zero in K_{1j}.

(ii) As follows from Table 3.4.3.4, one can always find a twinning operation that is either inversion, or a twofold axis or a mirror plane with a prominent crystallographic orientation. By applying the method of direct inspection (see Section 1.1.4.6.3), one can in most cases easily find morphic Cartesian components in the second domain state of the domain pair considered and prove that they differ only in sign.

Example 3.4.3.4. Tensor distinction of domains and switching in lead germanate. Lead germanate ($Pb_5Ge_3O_{11}$) undergoes a phase transition with symmetry descent $G = \bar{6} \supset 3 = F_1$ for which we find in Table 3.4.2.7, column K_{1j}, just one twinning group $K_{1j} = \bar{6}^\star$, *i.e.* $K^\star_{1j} = G$. This means that there is only one G-orbit of domain pairs. Since Fam3 = Fam$\bar{6}$ [see Table 3.4.2.2 and equation (3.4.3.40)] this orbit comprises non-ferroelastic domain pairs. In Table 3.4.3.4, we find for $F_1 = 3$ and $F^\star_{1j} = \bar{6}$ that the two domain states differ in some components of all property tensors listed in this table. The first polar tensor is the spontaneous polarization (the pair is ferroelectric) with one component ($a = 1$) that has opposite sign in the two domain states. In Table 3.1.3.1, we find for $G(= K_{1j}) = \bar{6}$ and $F_1 = 3$ that this component is $P_3 = P_z$. From Table 3.4.3.1, it follows that the state shift is electrically first order with switching field $\mathbf{E} = (0, 0, E_z)$.

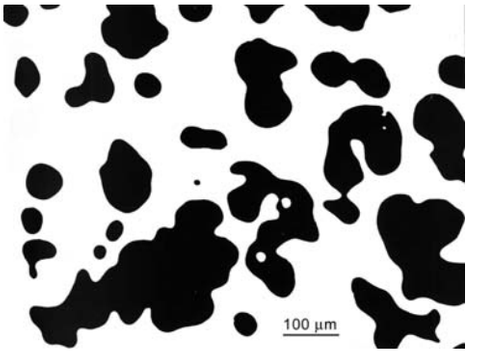

Fig. 3.4.3.3. Domain structure in lead germanate observed using a polarized-light microscope. Visualization based on the opposite sign of the optical activity coefficient in the two domain states. Courtesy of Vl. Shur, Ural State University, Ekaterinburg.

The first optical tensor, which could enable the visualization of the domain states, is the optical activity g_μ with two independent components which have opposite sign in the two domain states. In the software *GI★KoBo*-1, path: *Subgroups\View\Domains* or in Kopský (2001) we find these components: $g_3, g_1 + g_2$. Shur *et al.* (1989) have visualized in this way the domain structure of lead germanate with excellent black and white contrast (see Fig. 3.4.3.3). Other examples are given in Shuvalov & Ivanov (1964) and especially in Koňák *et al.* (1978).

Table 3.4.3.4 can be used readily for twinning by merohedry [see Chapter 3.3 and *e.g.* Cahn (1954); Koch (2004)], where it enables an easy determination of the tensor distinction of twin components and the specification of external fields for possible switching and detwinning.

Example 3.4.3.5. Tensor distinction and switching of Dauphiné twins in quartz. Quartz undergoes a phase transition from $G = 6_z2_x2_y$ to $F_1 = 3_z2_x$. Using the same procedure as in the previous example, we come to following conclusions: There are only two domain states $\mathbf{S}_1$, $\mathbf{S}_2$ and the twinning group, expressing the twin law, is equal to the high-symmetry group $K^\star_{12} = 6_z2_x2_z$. In Table 3.4.3.4, we find that these two states differ in one independent component of the piezoelectric tensor and in one elastic compliance component. Comparison of the matrices for $6_z2_x2_y$ and 3_z2_x (see Sections 1.1.4.10.3 and 1.1.4.10.4) yields the following morphic tensor components in the first domain state $\mathbf{S}_1$: $d^{(1)}_{11} = -d^{(1)}_{12} = -2d^{(1)}_{26}$ and $s^{(1)}_{14} = -s^{(1)}_{24} = 2s^{(1)}_{56}$. According to the rule given above, the values of morphic components in the second domain state $\mathbf{S}_2$ are $d^{(2)}_{11} = -d^{(1)}_{11} = -d^{(2)}_{12} = d^{(1)}_{12} = -2d^{(2)}_{26} = 2d^{(1)}_{26}$ and $s^{(2)}_{14} = -s^{(1)}_{14} = -s^{(2)}_{24} = s^{(1)}_{24} = 2s^{(2)}_{56} = -2s^{(1)}_{56}$ [see Section 3.4.5 (Glossary)]. These results show that there is an elastic state shift of second order and an electromechanical state shift of second order. Nonzero components $d_{14} = -d_{25}$ in $6_z2_x2_y$ are the same in both domain states. Similarly, one can find five independent components of the tensor $s_{\mu\nu}$ that are nonzero in $6_z2_x2_y$ and equal in both domain states. For the piezo-optic tensor $\pi_{\mu\nu}$, one can proceed in a similar way. Aizu (1973) has used the ferrobielastic character of the domain pairs for visualizing domains and realizing switching in quartz. Other methods for switching and visualizing domains in quartz are known (see *e.g.* Bertagnolli *et al.*, 1978, 1979).

3.4.3.6. *Ferroelastic domain pairs*

A *ferroelastic domain pair* consists of two domain states that have different spontaneous strain. A domain pair $(\mathbf{S}_1, \mathbf{S}_j)$ is a ferroelastic domain pair if the crystal family of its twinning group

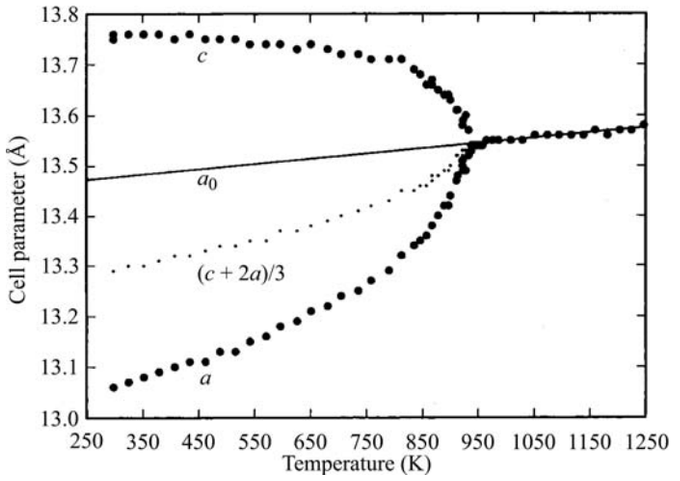

Fig. 3.4.3.4. Temperature dependence of lattice parameters in leucite. Courtesy of E. K. H Salje, University of Cambridge.

K_{1j} differs from the crystal family of the symmetry group F_1 of domain state $\mathbf{S}_1$,

$$\mathrm{Fam}K_{1j} \neq \mathrm{Fam}F_1. \qquad (3.4.3.43)$$

Before treating compatible domain walls and disorientations, we explain the basic concept of spontaneous strain.

3.4.3.6.1. *Spontaneous strain*

A *strain* describes a *change* of crystal shape (in a macroscopic description) or a change of the unit cell (in a microscopic description) under the influence of mechanical stress, temperature or electric field. If the relative changes are small, they can be described by a second-rank symmetric tensor $\mathbf{u}$ called the *Lagrangian strain*. The values of the strain components u_{ik}, $i,k = 1,2,3$ (or in matrix notation u_μ, $\mu = 1,\ldots,6$) can be calculated from the 'undeformed' unit-cell parameters before deformation and 'deformed' unit-cell parameters after deformation (see Schlenker *et al.*, 1978; Salje, 1990; Carpenter *et al.*, 1998).

A *spontaneous strain* describes the change of an 'undeformed' unit cell of the high-symmetry phase into a 'deformed' unit cell of the low-symmetry phase. To exclude changes connected with thermal expansion, one demands that the parameters of the undeformed unit cell are those that the high-symmetry phase would have at the temperature at which parameters of the low-symmetry phase are measured. To determine these parameters directly is not possible, since the parameters of the high-symmetry phase can be measured only in the high-symmetry phase. One uses, therefore, different procedures in order to estimate values for the high-symmetry parameters under the external conditions to which the measured values of the low-symmetry phase refer (see *e.g.* Salje, 1990; Carpenter *et al.*, 1998). Three main strategies are illustrated using the example of leucite (see Fig. 3.4.3.4):

(i) The lattice parameters of the high-symmetry phase are extrapolated from values measured in the high-symmetry phase (a straight line a_0 in Fig. 3.4.3.4). This is a preferred approach.

(ii) For certain symmetry descents, it is possible to approximate the high-symmetry parameters in the low-symmetry phase by average values of the lattice parameters in the low-symmetry phase. Thus for example in cubic $\rightarrow$ tetragonal transitions one can take for the cubic lattice parameter $a_0 = (2a + c)/3$ (the dotted curve in Fig. 3.4.3.4), for cubic $\rightarrow$ orthorhombic transitions one may assume $a_0 = (abc)^{1/3}$, where a, b, c are the lattice parameters of the low-symmetry phase. Errors are introduced if there is a significant volume strain, as in leucite.

(iii) Thermal expansion is neglected and for the high-symmetry parameters in the low-symmetry phase one takes the lattice parameters measured in the high-symmetry phase as close as possible to the transition. This simplest method gives better results than average values in leucite, but in general may lead to significant errors.

Spontaneous strain has been examined in detail in many ferroic crystals by Carpenter *et al.* (1998).

Spontaneous strain can be divided into two parts: one that is different in all ferroelastic domain states and the other that is the same in all ferroelastic domain states. This division can be achieved by introducing a *modified strain tensor* (Aizu, 1970*b*), also called a *relative spontaneous strain* (Wadhawan, 2000):

$$\mathbf{u}^{(i)}_{(s)} = \mathbf{u}^{(i)} - \mathbf{u}^{(\mathrm{av})}_{(s)}, \qquad (3.4.3.44)$$

where $\mathbf{u}^{(i)}_{(s)}$ is the matrix of relative (modified) spontaneous strain in the ferroelastic domain state $\mathbf{R}_i$, $\mathbf{u}^{(i)}$ is the matrix of an 'absolute' spontaneous strain in the same ferroelastic domain state $\mathbf{R}_i$ and $\mathbf{u}^{(\mathrm{av})}_{(s)}$ is the matrix of an *average spontaneous strain* that is equal to the sum of the matrices of absolute spontaneous strains over all n_a ferroelastic domain states,

$$\mathbf{u}^{(\mathrm{av})} = \frac{1}{n_a}\sum_{j=1}^{n_a}\mathbf{u}^{(j)}. \qquad (3.4.3.45)$$

The relative spontaneous strain $\mathbf{b}^{(i)}_{(s)}$ is a *symmetry-breaking strain* that transforms according to a non-identity representation of the parent group G, whereas the average spontaneous strain is a *non-symmetry breaking strain* that transforms as the identity representation of G.

Example 3.4.3.6. We illustrate these concepts with the example of symmetry descent $4_z/m_z m_x m_{xy} \supset 2_x m_y m_z$ with two ferroelastic domain states $\mathbf{R}_1$ and $\mathbf{R}_2$ (see Fig. 3.4.2.2). The absolute spontaneous strain in the first ferroelastic domain state $\mathbf{R}_1$ is

$$\mathbf{u}^{(1)} = \begin{pmatrix} \frac{a-a_0}{a_0} & 0 & 0 \\ 0 & \frac{b-a_0}{a_0} & 0 \\ 0 & 0 & \frac{c-c_0}{c_0} \end{pmatrix} = \begin{pmatrix} u_{11} & 0 & 0 \\ 0 & u_{22} & 0 \\ 0 & 0 & u_{33} \end{pmatrix}, \qquad (3.4.3.46)$$

where a, b, c and a_0, b_0, c_0 are the lattice parameters of the orthorhombic and tetragonal phases, respectively.

The spontaneous strain $\mathbf{u}^{(2)}$ in domain state $\mathbf{R}_2$ is obtained by applying to $\mathbf{u}^{(1)}$ any switching operation that transforms $\mathbf{R}_1$ into $\mathbf{R}_2$ (see Table 3.4.2.1),

$$\mathbf{u}^{(2)} = \begin{pmatrix} u_{22} & 0 & 0 \\ 0 & u_{11} & 0 \\ 0 & 0 & u_{33} \end{pmatrix}. \qquad (3.4.3.47)$$

The average spontaneous strain is, according to equation (3.4.3.45),

$$\mathbf{u}^{(\mathrm{av})} = \tfrac{1}{2}\begin{pmatrix} u_{11}+u_{22} & 0 & 0 \\ 0 & u_{11}+u_{22} & 0 \\ 0 & 0 & u_{33}+u_{33} \end{pmatrix}. \qquad (3.4.3.48)$$

This deformation is invariant under any operation of G.

The relative spontaneous strains in ferroelastic domain states $\mathbf{R}_1$ and $\mathbf{R}_2$ are, according to equation (3.4.3.44),

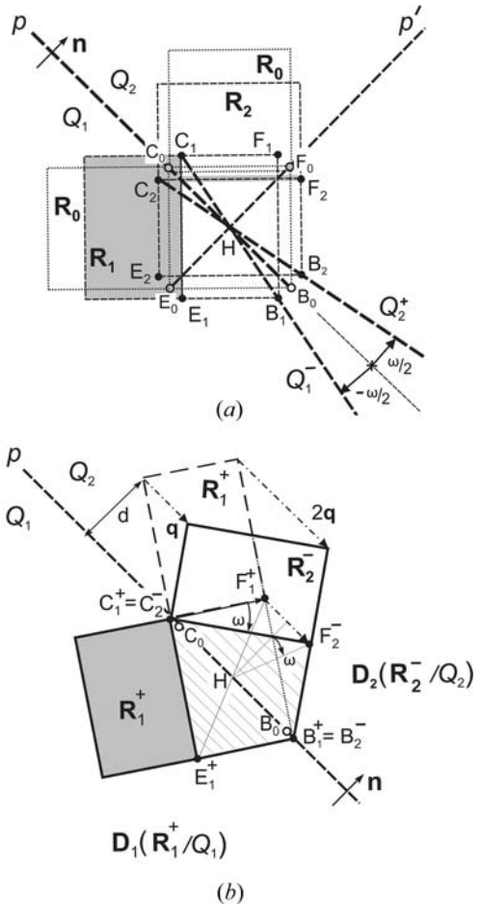

Fig. 3.4.3.5. Two ways of constructing a ferroelastic domain twin. (*a*) Formation of ferroelastic single-domain states $\mathbf{R}_1$, $\mathbf{R}_2$ from the parent phase state $\mathbf{R}_0$ and then rotating away these single-domain states through an angle $\pm\frac{1}{2}\omega$ about the domain-pair axis H so that disoriented ferroelastic domain states $\mathbf{R}_1^+$ and $\mathbf{R}_2^-$ meet along one of two perpendicular planes of equal deformation p or p'. (*b*) Formation of a ferroelastic twin from one ferroelastic domain state $\mathbf{R}_1^+$ by a simple shear deformation with a shear angle (obliquity) ω. For more details see the text.

$$\mathbf{u}_{(s)}^{(1)} = \mathbf{u}^{(1)} - \mathbf{u}^{(\mathrm{av})} = \begin{pmatrix} \frac{1}{2}(u_{11}-u_{22}) & 0 & 0 \\ 0 & -\frac{1}{2}(u_{11}-u_{22}) & 0 \\ 0 & 0 & 0 \end{pmatrix}, \tag{3.4.3.49}$$

$$\mathbf{u}_{(s)}^{(2)} = \mathbf{u}^{(2)} - \mathbf{u}^{(\mathrm{av})} = \begin{pmatrix} -\frac{1}{2}(u_{11}-u_{22}) & 0 & 0 \\ 0 & \frac{1}{2}(u_{11}-u_{22}) & 0 \\ 0 & 0 & 0 \end{pmatrix}. \tag{3.4.3.50}$$

Symmetry-breaking nonzero components of the relative spontaneous strain are identical, up to the factor $\frac{1}{2}$, with the secondary tensor parameters $\lambda_b^{(1)}$ and $\lambda_b^{(2)}$ of the transition $4_z/m_z m_x m_{xy} \supset 2_x m_y m_z$ with the stabilizer $I_{4_z/m_z m_x m_{xy}}(\mathbf{R}_1) = I_{4_z/m_z m_x m_{xy}}(\mathbf{R}_2) = m_x m_y m_z$. The non-symmetry-breaking component u_{33} does not appear in the relative spontaneous strain.

The form of relative spontaneous strains for all ferroelastic domain states of all full ferroelastic phases are listed in Aizu (1970*b*).

3.4.3.6.2. *Equally deformed planes of a ferroelastic domain pair*

We start with the example of a phase transition with the symmetry descent $G = 4_z/m_z m_x m_{xy} \supset 2_x m_y m_z$, which generates two ferroelastic single-domain states $\mathbf{R}_1$ and $\mathbf{R}_2$ (see Fig. 3.4.2.2). An 'elementary cell' of the parent phase is represented in Fig. 3.4.3.5(*a*) by a square $B_0E_0C_0F_0$ and the corresponding domain state is denoted by $\mathbf{R}_0$.

In the ferroic phase, the square $B_0E_0C_0F_0$ can change either under spontaneous strain $\mathbf{u}^{(1)}$ into a spontaneously deformed rectangular cell $B_1E_1C_1F_1$ representing a domain state $\mathbf{R}_1$, or under a spontaneous strain $\mathbf{u}^{(2)}$ into rectangular $B_2E_2C_2F_2$ representing domain state $\mathbf{R}_2$. We shall use the letter $\mathbf{R}_0$ as a symbol of the parent phase and $\mathbf{R}_1$, $\mathbf{R}_2$ as symbols of two ferroelastic single-domain states.

Let us now choose in the parent phase a vector $\overrightarrow{HB_0}$. This vector changes into $\overrightarrow{HB_1}$ in ferroelastic domain state $\mathbf{R}_1$ and into $\overrightarrow{HB_2}$ in ferroelastic domain state $\mathbf{R}_1$. We see that the resulting vectors $\overrightarrow{HB_1}$ and $\overrightarrow{HB_2}$ have different direction but equal length: $|\overrightarrow{HB_1}| = |\overrightarrow{HB_2}|$. This consideration holds for any vector in the plane p, which can therefore be called an *equally deformed plane* (EDP). One can find that the perpendicular plane p' is also an equally deformed plane, but there is no other plane with this property.

The intersection of the two perpendicular equally deformed planes p and p' is a line called an *axis of the ferroelastic domain pair* ($\mathbf{R}_1$, $\mathbf{R}_2$) (in Fig. 3.4.3.5 it is a line at H perpendicular to the paper). This axis is the only line in which any vector chosen in the parent phase exhibits equal deformation and has its direction unchanged in both single-domain states $\mathbf{R}_1$ and $\mathbf{R}_2$ of a ferroelastic domain pair.

This consideration can be expressed analytically as follows (Fousek & Janovec, 1969; Sapriel, 1975). We choose in the parent phase a plane p and a unit vector $\mathbf{v}(x_1, x_2, x_3)$ in this plane. The changes of lengths of this vector in the two ferroelastic domain states $\mathbf{R}_1$ and $\mathbf{R}_2$ are $u_{ik}^{(1)}x_ix_k$ and $u_{ik}^{(2)}x_ix_k$, respectively, where $u_{ik}^{(1)}$ and $u_{ik}^{(2)}$ are spontaneous strains in $\mathbf{R}_1$ and $\mathbf{R}_2$, respectively (see *e.g.* Nye, 1985). (We are using the Einstein summation convention: when a letter suffix occurs twice in the same term, summation with respect to that suffix is to be understood.) If these changes are equal, *i.e.* if

$$u_{ik}^{(1)}x_ix_k = u_{ik}^{(2)}x_ix_k, \tag{3.4.3.51}$$

for any vector $\mathbf{v}(x_1, x_2, x_3)$ in the plane p, then this plane will be an equally deformed plane. If we introduce a *differential spontaneous strain*

$$\Delta u_{ik} \equiv u_{ik}^{(2)} - u_{ik}^{(1)}, \quad i,k = 1,2,3, \tag{3.4.3.52}$$

the condition (3.4.3.51) can be rewritten as

$$\Delta u_{ik}x_ix_j = 0. \tag{3.4.3.53}$$

This equation describes a cone with the apex at the origin. The cone degenerates into two planes if the determinant of the differential spontaneous strain tensor equals zero,

$$\det\Delta u_{ik} = 0. \tag{3.4.3.54}$$

If this condition is satisfied, two solutions of (3.4.3.53) exist:

$$Ax_1 + Bx_2 + Cx_3 = 0, \quad A'x_1 + B'x_2 + C'x_3 = 0. \tag{3.4.3.55}$$

These are equations of two planes p and p' passing through the origin. Their normal vectors are $\mathbf{n} = [ABC]$ and $\mathbf{n}' = [A'B'C']$. It can be shown that from the equation

$$\Delta u_{11} + \Delta u_{22} + \Delta u_{33} = 0, \tag{3.4.3.56}$$

which holds for the trace of the matrix $\det\Delta u_{ik}$, it follows that these two planes are perpendicular:

$$AA' + BB' + CC' = 0. \tag{3.4.3.57}$$

The intersection of these equally deformed planes (3.4.3.53) is the *axis* $\mathbf{h}$ *of the ferroelastic domain pair* ($\mathbf{R}_1$, $\mathbf{R}_2$).

Let us illustrate the application of these results to the domain pair $(\mathbf{R}_1, \mathbf{R}_2)$ depicted in Fig. 3.4.3.1(b) and discussed above. From equations (3.4.3.41) and (3.4.3.47), or (3.4.3.49) and (3.4.3.50) we find the only nonzero components of the difference strain tensor are

$$\Delta u_{11} = u_{22} - u_{11}, \quad \Delta u_{22} = u_{11} - u_{22}. \tag{3.4.3.58}$$

Condition (3.4.3.54) is fulfilled and equation (3.4.3.53) is

$$\Delta u_{11} x_1^2 + \Delta u_{22} x_2^2 = (u_{22} - u_{11}) x_1^2 + (u_{11} - u_{22}) x_2^2 = 0. \tag{3.4.3.59}$$

There are two solutions of this equation:

$$x_1 = x_2, \quad x_1 = -x_2. \tag{3.4.3.60}$$

These two equally deformed planes p and p' have the normal vectors $\mathbf{n} = [\bar{1}10]$ and $\mathbf{n}' = [110]$. The axis $\mathbf{h}$ of this domain pair is directed along [001].

Equally deformed planes in our example have the same orientations as have the mirror planes $m_{\bar{x}y}$ and m_{xy} lost at the transition $4_z/m_z m_x m_{xy} \supset m_x m_y m_z$. From Fig. 3.4.3.5($a$) it is clear why: reflection $m_{\bar{x}y}$, which is a transposing operation of the domain pair $(\underrightarrow{\mathbf{R}_1}, \mathbf{R}_2)$, ensures that the vectors $\overrightarrow{HB_1}$ and $\overrightarrow{HB_2}$ arising from HB_0 have equal length. A similar conclusion holds for a 180° rotation and a plane perpendicular to the corresponding twofold axis. Thus we come to two useful rules:

Any reflection through a plane that is a transposing operation of a ferroelastic domain pair ensures the existence of two planes of equal deformation: one is parallel to the corresponding mirror plane and the other one is perpendicular to this mirror plane.

Any 180° rotation that is a transposing operation of a ferroelastic domain pair ensures the existence of two equally deformed planes: one is perpendicular to the corresponding twofold axis and the other one is parallel to this axis.

A reflection in a plane or a 180° rotation generates at least one equally deformed plane with a fixed prominent *crystallographic orientation* independent of the magnitude of the spontaneous strain; the other perpendicular equally deformed plane may have a *non-crystallographic orientation* which depends on the spontaneous strain and changes with temperature. If between switching operations there are two reflections with corresponding perpendicular mirror planes, or two 180° rotations with corresponding perpendicular twofold axes, or a reflection and a 180° rotation with a corresponding twofold axis parallel to the mirror, then both perpendicular equally deformed planes have fixed crystallographic orientations. If there are no switching operations of the second order, then both perpendicular equally deformed planes may have non-crystallographic orientations, or equally deformed planes may not exist at all.

Equally deformed planes in ferroelastic–ferroelectric phases have been tabulated by Fousek (1971). Sapriel (1975) lists equations (3.4.3.55) of equally deformed planes for all ferroelastic phases. Table 3.4.3.6 contains the orientation of equally deformed planes (with further information about the walls) for representative domain pairs of all orbits of ferroelastic domain pairs. Table 3.4.3.7 lists representative domain pairs of all ferroelastic orbits for which no compatible walls exist.

3.4.3.6.3. *Disoriented domain states, ferroelastic domain twins and their twin laws*

To examine another possible way of forming a ferroelastic domain twin, we return once again to Fig. 3.4.3.5(a) and split the space along the plane p into a half-space Q_1 on the negative side of the plane p (defined by a negative end of normal $\mathbf{n}$) and another half-space Q_2 on the positive side of p. In the parent phase, the whole space is filled with domain state $\mathbf{R}_0$ and we can, therefore, treat the crystal in region Q_1 as a domain $\mathbf{D}_1(\mathbf{R}_0, Q_1)$ and the crystal in region Q_2 as a domain $\mathbf{D}_2(\mathbf{R}_0, Q_2)$ (we remember that a domain is specified by its domain region, *e.g.* Q_1, and by a domain state, *e.g.* $\mathbf{R}_1$, in this region; see Section 3.4.2.1).

Now we cool the crystal down and exert the spontaneous strain $\mathbf{u}^{(1)}$ on domain $\mathbf{D}_1(\mathbf{R}_0, Q_1)$. The resulting domain $\mathbf{D}_1(\mathbf{R}_1, Q_1^-)$ contains domain state $\mathbf{R}_1$ in the domain region Q_1^- with the planar boundary along $(\overline{B_1 C_1})$ (the overbar '$-$' signifies a rotation of the boundary in the positive sense). Similarly, domain $\mathbf{D}_2(\mathbf{R}_0, Q_2)$ changes after performing spontaneous strain $\mathbf{u}^{(2)}$ into domain $\mathbf{D}_2(\mathbf{R}_2, Q_2^+)$ with domain state $\mathbf{R}_2$ and the planar boundary along $(\overline{B_2 C_2})$. This results in a disruption in the sector $B_1 A B_2$ and in an overlap of $\mathbf{R}_1$ and $\mathbf{R}_2$ in the sector $C_1 A C_2$.

The overlap can be removed and the continuity recovered by rotating the domain $\mathbf{D}_1(\mathbf{R}_1, Q_1^-)$ through angle $\omega/2$ and the domain $\mathbf{D}_2(\mathbf{R}_2, Q_2^+)$ through $-\omega/2$ about the domain-pair axis A (see Fig. 3.4.3.5a and b). This rotation changes the domain $\mathbf{D}_1(\mathbf{R}_1, Q_1^-)$ into domain $\mathbf{D}_1(\mathbf{R}_1^+, Q_1)$ and domain $\mathbf{D}_2(\mathbf{R}_2, Q_2^-)$ into domain $\mathbf{D}_1(\mathbf{R}_2^-, Q_2)$, where $\mathbf{R}_1^+$ and $\mathbf{R}_2^-$ are domain states rotated away from the single-domain state orientation through $\omega/2$ and $-\omega/2$, respectively. Domains $\mathbf{D}_1(\mathbf{R}_1, Q_1)$ and $\mathbf{D}_1(\mathbf{R}_2, Q_2)$ meet without additional strains or stresses along the plane p and form a *simple ferroelastic twin* with a *compatible domain wall* along p. This wall is stress-free and fulfils the conditions of mechanical compatibility.

Domain states $\mathbf{R}_1^+$ and $\mathbf{R}_2^-$ with new orientations are called *disoriented (misoriented) domain states* or *suborientational states* (Shuvalov *et al.*, 1985; Dudnik & Shuvalov, 1989) and the angles $\omega/2$ and $-\omega/2$ are the *disorientation angles* of $\mathbf{R}_1^+$ and $\mathbf{R}_2^-$, respectively.

We have described the formation of a ferroelastic domain twin by rotating single-domain states into new orientations in which a stress-free compatible contact of two ferroelastic domains is achieved. The advantage of this theoretical construct is that it provides a visual interpretation of disorientations and that it works with ferroelastic single-domain states which can be easily derived and transformed.

There is an alternative approach in which a domain state in one domain is produced from the domain state in the other domain by a shear deformation. The same procedure is used in mechanical twinning [for mechanical twinning, see Section 3.3.8.4 and *e.g.* Cahn (1954); Klassen-Neklyudova (1964); Christian (1975)].

We illustrate this approach again using our example. From Fig. 3.4.3.5(b) it follows that domain state $\mathbf{R}_2^-$ in the second domain can be obtained by performing a simple shear on the domain state $\mathbf{R}_1^+$ of the first domain. In this simple shear, a point is displaced in a direction parallel to the equally deformed plane p (in mechanical twinning called a *twin plane*) and to a plane perpendicular to the axis of the domain pair (*plane of shear*). The displacement $\mathbf{q}$ is proportional to the distance d of the point from the domain wall. The *amount of shear* is measured either by the absolute value of this displacement at a unit distance, $s = q/d$, or by an angle ω called a *shear angle* (sometimes 2ω is defined as the shear angle). There is no change of volume connected with a simple shear.

The angle ω is also called an *obliquity* of a twin (Cahn, 1954) and is used as a convenient measure of pseudosymmetry of the ferroelastic phase.

The high-resolution electron microscopy image in Fig. 3.4.3.6 reveals the relatively large shear angle (obliquity) ω of a ferroelastic twin in the monoclinic phase of tungsten trioxide (WO_3). The plane (101) corresponds to the plane p of a ferroelastic wall in Fig. 3.4.3.5(b). The planes $(\bar{1}01)$ are crystallographic planes in the lower and upper ferroelastic domains, which correspond in Fig. 3.4.3.5(b) to domain $\mathbf{D}_1(\mathbf{R}_1^+, Q_1)$ and domain $\mathbf{D}_2(\mathbf{R}_2^-, Q_2)$, respectively. The planes $(\bar{1}01)$ in these domains correspond to the diagonals of the elementary cells of $\mathbf{R}_1^+$ and $\mathbf{R}_2^-$ in Fig. 3.4.3.5(b) and are nearly perpendicular to the wall. The

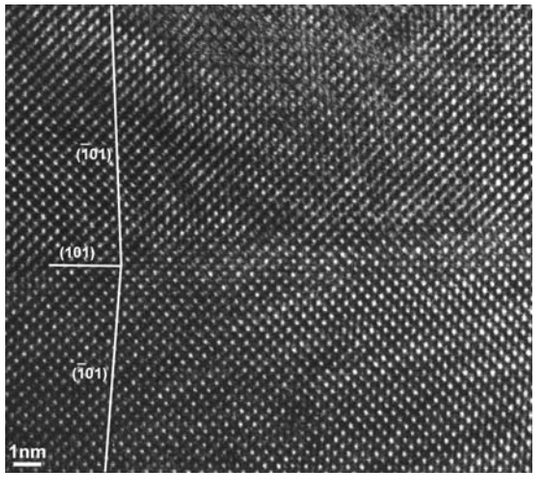

Fig. 3.4.3.6. High-resolution electron microscopy image of a ferroelastic twin in the orthorhombic phase of WO_3. Courtesy of H. Lemmens, EMAT, University of Antwerp.

angle between these planes equals 2ω, where ω is the shear angle (obliquity) of the ferroelastic twin.

Disorientations of domain states in a ferroelastic twin bring about a deviation of the optical indicatrix from a strictly perpendicular position. Owing to this effect, ferroelastic domains exhibit different colours in polarized light and can be easily visualized. This is illustrated for a domain structure of $YBa_2Cu_3O_{7-\delta}$ in Fig. 3.4.3.7. The symmetry descent $G = 4_z/m_z m_x m_{xy} \supset m_x m_y m_z = F_1 = F_2$ gives rise to two ferroelastic domain states $\mathbf{R}_1$ and $\mathbf{R}_2$. The twinning group K_{12} of the non-trivial domain pair $(\mathbf{R}_1, \mathbf{R}_2)$ is

$$K_{12}[m_x m_y m_z] = J_{12}^{\star} = m_x m_y m_z \cup 4_z^{\star}\{2_x m_y m_z\} = 4_z^{\star}/m_z m_x m_{xy}^{\star}. \tag{3.4.3.61}$$

The colour of a domain state observed in a polarized-light microscope depends on the orientation of the index ellipsoid (indicatrix) with respect to a fixed polarizer and analyser. This index ellipsoid transforms in the same way as the tensor of spontaneous strain, *i.e.* it has different orientations in ferroelastic domain states. Therefore, different ferroelastic domain states exhibit different colours: in Fig. 3.4.3.7, the blue and pink areas (with different orientations of the ellipse representing the spontaneous strain in the plane of of figure) correspond to two different ferroelastic domain states. A rotation of the crystal that does not change the orientation of ellipses (*e.g.* a 180° rotation about an axis parallel to the fourfold rotation axis) does not change the colours (ferroelastic domain states). If one neglects disorientations of ferroelastic domain states (see Section 3.4.3.6) – which are too small to be detected by polarized-light microscopy – then none of the operations of the group $F_1 = F_2 = m_x m_y m_z$ change the single-domain ferroelastic domain states $\mathbf{R}_1$, $\mathbf{R}_2$, hence there is no change in the colours of domain regions of the crystal. On the other hand, all operations with a star symbol (operations lost at the transition) exchange domain states $\mathbf{R}_1$ and $\mathbf{R}_2$, *i.e.* also exchange the two colours in the domain regions. The corresponding permutation is a transposition of two colours and this attribute is represented by a star attached to the symbol of the operation. This exchange of colours is nicely demonstrated in Fig. 3.4.3.7 where a $-90°$ rotation is accompanied by an exchange of the pink and blue colours in the domain regions (Schmid, 1991, 1993).

It can be shown (Shuvalov *et al.*, 1985; Dudnik & Shuvalov, 1989) that for small spontaneous strains the amount of shear s and the angle ω can be calculated from the second invariant Λ_2 of the differential tensor Δu_{ik}:

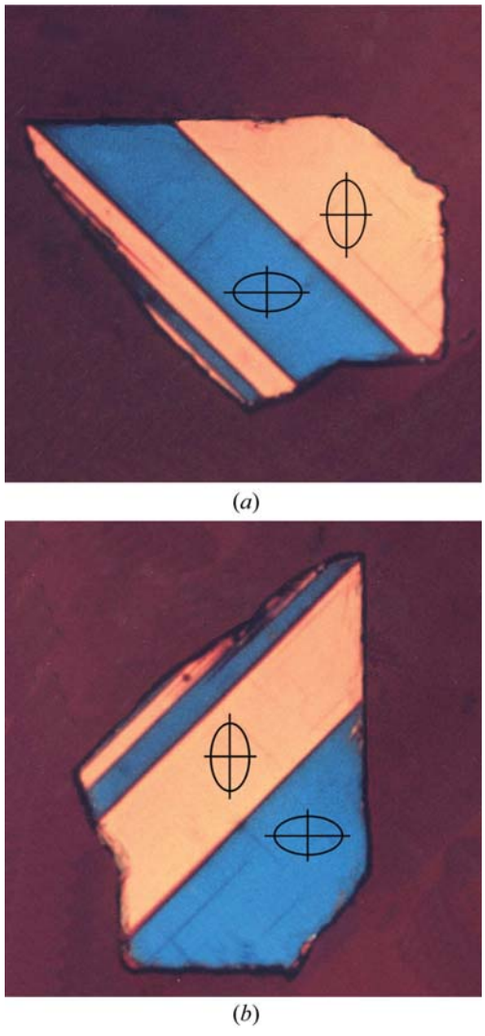

Fig. 3.4.3.7. Ferroelastic twins in a very thin $YBa_2Cu_3O_{7-\delta}$ crystal observed in a polarized-light microscope. Courtesy of H. Schmid, Université de Geneve.

$$s = 2\sqrt{-\Lambda_2}, \tag{3.4.3.62}$$

$$\omega = \sqrt{-\Lambda_2}, \tag{3.4.3.63}$$

where

$$\Lambda_2 = \begin{vmatrix} \Delta u_{11} & \Delta u_{12} \\ \Delta u_{21} & \Delta u_{22} \end{vmatrix} + \begin{vmatrix} \Delta u_{22} & \Delta u_{23} \\ \Delta u_{32} & \Delta u_{33} \end{vmatrix} + \begin{vmatrix} \Delta u_{11} & \Delta u_{13} \\ \Delta u_{31} & \Delta u_{33} \end{vmatrix}. \tag{3.4.3.64}$$

In our example, where there are only two nonzero components of the differential spontaneous strain tensor [see equation (3.4.3.58)], the second invariant $\Lambda_2 = -(\Delta u_{11}\Delta u_{22}) = -(u_{22} - u_{11})^2$ and the angle ω is

$$\omega = \pm|u_{22} - u_{11}|. \tag{3.4.3.65}$$

In this case, the angle ω can also be expressed as $\omega = \pi/2 - 2\arctan a/b$, where a and b are lattice parameters of the orthorhombic phase (Schmid *et al.*, 1988).

The shear angle ω ranges in ferroelastic crystals from minutes to degrees (see *e.g.* Schmid *et al.*, 1988; Dudnik & Shuvalov, 1989).

Each equally deformed plane gives rise to two compatible domain walls of the same orientation but with opposite sequence of domain states on each side of the plane. We shall use for a *simple domain twin* with a planar wall a symbol $(\mathbf{R}_1^+|\mathbf{n}|\mathbf{R}_2^-)$ in which $\mathbf{n}$ denotes the normal to the wall. The bra–ket symbol (| and |) represents the half-space domain regions on the negative

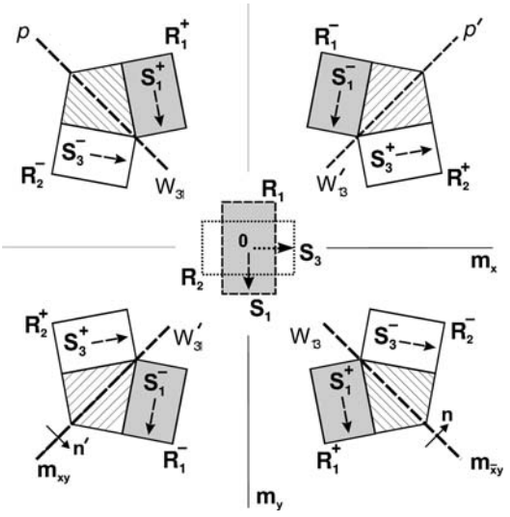

Fig. 3.4.3.8. Exploded view of four ferroelastic twins with disoriented ferroelastic domain states $\mathbf{R}_1^+$, $\mathbf{R}_2^-$ and $\mathbf{R}_1^-$, $\mathbf{R}_2^+$ formed from a single-domain pair ($\mathbf{S}_1$, $\mathbf{S}_2$) (in the centre).

and positive sides of $\mathbf{n}$, respectively, for which we have used letters Q_1 and Q_2, respectively. Then ($\mathbf{R}_1^+|$ and $|\mathbf{R}_2^-$) represent domains $\mathbf{D}_1(\mathbf{R}_1^+, Q_1)$ and $\mathbf{D}_2(\mathbf{R}_2^-, Q_2)$, respectively. The symbol ($\mathbf{R}_1^+|\mathbf{R}_2^-$) properly specifies a domain twin with a zero-thickness domain wall.

A domain wall can be considered as a domain twin with domain regions restricted to non-homogeneous parts near the plane p. For a domain wall in domain twin ($\mathbf{R}_1^+|\mathbf{R}_2^-$) we shall use the symbol [$\mathbf{R}_1^+|\mathbf{R}_2^-$], which expresses the fact that a domain wall of zero thickness needs the same specification as the domain twin.

If we exchange domain states in the twin ($\mathbf{R}_1^+|\mathbf{n}|\mathbf{R}_2^-$), we get a *reversed twin (wall)* with the symbol ($\mathbf{R}_2^-|\mathbf{n}|\mathbf{R}_1^+$). These two ferroelastic twins are depicted in the lower right and upper left parts of Fig. 3.4.3.8, where – for ferroelastic–non-ferroelectric twins – we neglect spontaneous polarization of ferroelastic domain states. The reversed twin $\mathbf{R}_2^-|\mathbf{n}'|\mathbf{R}_1^+$ has the opposite shear direction.

Twin and reversed twin can be, but may not be, crystallographically equivalent. Thus *e.g.* ferroelastic–non-ferroelectric twins ($\mathbf{R}_1^+|\mathbf{n}|\mathbf{R}_2^-$) and ($\mathbf{R}_2^-|\mathbf{n}|\mathbf{R}_1^+$) in Fig. 3.4.3.8 are equivalent, *e.g. via* 2_z, whereas ferroelastic–ferroelectric twins ($\mathbf{S}_1^+|\mathbf{n}|\mathbf{S}_3^-$) and ($\mathbf{S}_3^-|\mathbf{n}|\mathbf{S}_1^+$) are not equivalent, since there is no operation in the group K_{12} that would transform ($\mathbf{S}_1^+|\mathbf{n}|\mathbf{S}_3^-$) into ($\mathbf{S}_3^-|\mathbf{n}|\mathbf{S}_1^+$).

As we shall show in the next section, the symmetry group $\mathsf{T}_{12}(\mathbf{n})$ of a twin and the symmetry group $\mathsf{T}_{21}(\mathbf{n})$ of a reverse twin are equal,

$$\mathsf{T}_{12}(\mathbf{n}) = \mathsf{T}_{21}(\mathbf{n}). \tag{3.4.3.66}$$

A sequence of repeating twins and reversed twins

$$\ldots \mathbf{R}_1^+|\mathbf{n}|\mathbf{R}_2^-|\mathbf{n}|\mathbf{R}_1^+|\mathbf{n}|\mathbf{R}_2^-|\mathbf{n}|\mathbf{R}_1^+|\mathbf{n}|\mathbf{R}_2^-|\mathbf{n}|\mathbf{R}_1^+|\mathbf{n}|\mathbf{R}_2^- \ldots \tag{3.4.3.67}$$

forms a *lamellar ferroelastic domain structure* that is very common in ferroelastic phases (see *e.g.* Figs. 3.4.1.1 and 3.4.1.4).

Similar considerations can be applied to the second equally deformed plane p' that is perpendicular to p. The two twins and corresponding compatible domain walls for the equally deformed plane p' have the symbols ($\mathbf{R}_1^-|\mathbf{n}'|\mathbf{R}_2^+$) and ($\mathbf{R}_2^-|\mathbf{n}'|\mathbf{R}_1^+$), and are also depicted in Fig. 3.4.3.8. The corresponding lamellar domain structure is

$$\ldots \mathbf{R}_1^-|\mathbf{n}'|\mathbf{R}_2^+|\mathbf{n}'|\mathbf{R}_1^-|\mathbf{n}'|\mathbf{R}_2^+|\mathbf{n}'|\mathbf{R}_1^-|\mathbf{n}'|\mathbf{R}_2^+|\mathbf{n}'|\mathbf{R}_1^-|\mathbf{n}'|\mathbf{R}_2^+ \ldots . \tag{3.4.3.68}$$

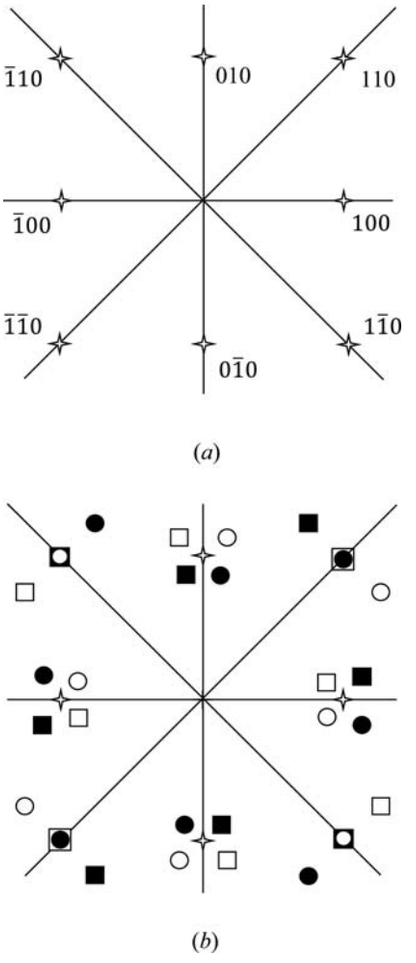

Fig. 3.4.3.9. Splitting of diffraction spots at a tetragonal-to-orthorhombic transition. (*a*) Fragment of the reciprocal lattice (stars) of the parent tetragonal phase. (*b*) Superposition of the reciprocal lattices of the four ferroelastic domains states in Fig. 3.4.3.8: $\mathbf{R}_1^+$ (reciprocal lattice black squares), $\mathbf{R}_1^-$ (reciprocal lattice black circles), $\mathbf{R}_2^+$ (reciprocal lattice white squares) and $\mathbf{R}_2^-$ (reciprocal lattice white circles).

Thus from one ferroelastic single-domain pair ($\mathbf{R}_1, \mathbf{R}_2$) depicted in the centre of Fig. 3.4.3.8 four different ferroelastic domain twins can be formed. It can be shown that these four twins have the same shear angle ω and the same amount of shear s. They differ only in the direction of the shear.

Four disoriented domain states $\mathbf{R}_1^-, \mathbf{R}_1^+$ and $\mathbf{R}_2^-, \mathbf{R}_2^+$ that appear in the four domain twins considered above are related by lost operations (*e.g.* diagonal, vertical and horizontal reflections), *i.e.* they are crystallographically equivalent. This result can readily be obtained if we consider the stabilizer of a disoriented domain state $\mathbf{R}_1^+$, which is $I_{4/mmm}(\mathbf{R}_1^+) = 2_z/m_z$. Then the number $n_a^{\rm dis}$ of disoriented ferroelastic domain states is given by

$$n_a^{\rm dis} = [G : I_g(\mathbf{R}_1^+)] = |4_z/m_z m_x m_{xy}| : |2_z/m_z] = 16 : 4 = 4. \tag{3.4.3.69}$$

All these domain states appear in ferroelastic polydomain structures that contain coexisting lamellar structures (3.4.3.67) and (3.4.3.68).

Disoriented domain states in ferroelastic domain structures can be recognized by diffraction techniques (*e.g.* using an X-ray precession camera). The presence of these four disoriented domain states results in splitting of the diffraction spots of the high-symmetry tetragonal phase into four or two spots in the orthorhombic ferroelastic phase. This splitting is schematically depicted in Fig. 3.4.3.9. For more details see *e.g.* Shmyt'ko *et al.* (1987), Rosová *et al.* (1993), and Rosová (1999).

Finally, we turn to *twin laws of ferroelastic domain twins with compatible domain walls*. In a ferroelastic twin, say $(\mathbf{R}_1^+|\mathbf{n}|\mathbf{R}_2^-)$, there are just two possible *twinning operations* that interchange two ferroelastic domain states $\mathbf{R}_1^+$ and $\mathbf{R}_2^-$ of the twin: reflection through the plane of the domain wall ($m_{xy}^\star$ in our example) and 180° rotation with a rotation axis in the intersection of the domain wall and the plane of shear ($2_{xy}^\star$). These are the only transposing operations of the domain pair $(\mathbf{R}_1, \mathbf{R}_2)$ that are preserved by the shear; all other transposing operations of the domain pair $(\mathbf{R}_1, \mathbf{R}_2)$ are lost. (This is a difference from non-ferroelastic twins, where all transposing operations of the pair become twinning operations of a non-ferroelastic twin.)

Consider the twin $(\mathbf{S}_1^+|\mathbf{n}|\mathbf{S}_3^-)$ in Fig. 3.4.3.8. By *non-trivial twinning operations* we understand transposing operations of the domain pair $(\mathbf{S}_1^+, \mathbf{S}_3^-)$, whereas *trivial twinning operations* leave invariant $\mathbf{S}_1^+$ and $\mathbf{S}_3^-$. As we shall see in the next section, the union of trivial and non-trivial twinning operations forms a group $\mathsf{T}_{1+2^-}(\mathbf{n})$. This group, called the *symmetry group of the twin* $(\mathbf{S}_1^+|\mathbf{n}|\mathbf{S}_3^-)$, comprises all symmetry operations of this twin and we shall use it for designating the *twin law of the ferroelastic twin*, just as the group $J_{1j}^\star$ of the domain pair $(\mathbf{S}_1, \mathbf{S}_j)$ specifies the twin law of a non-ferroelastic twin. This group $\mathsf{T}_{1+2^-}(\mathbf{n})$ is a layer group (see Section 3.4.4.2) that keeps the plane p invariant, but for characterizing the twin law, which specifies the relation of domain states of two domains in the twin, one can treat $\mathsf{T}_{1+2^-}(\mathbf{n})$ as an ordinary (dichromatic) point group $T_{1+2^-}(\mathbf{n})$. Thus the twin law of the domain twin $(\mathbf{S}_1^+|\mathbf{n}|\mathbf{S}_3^-)$ is designated by the group

$$T_{1+3^-}(\mathbf{n}) = 2_{xy}^\star m_{x\bar{y}}^\star m_z = T_{3^-1^+}(\mathbf{n}), \tag{3.4.3.70}$$

where (3.4.3.70) expresses the fact that a twin and the reversed twin have the same symmetry, see equation (3.4.3.66). We see that this group coincides with the symmetry group J_{1+2^-} of the single-domain pair $(\mathbf{S}_1, \mathbf{S}_3)$ (see Fig. 3.4.3.1*b*).

The twin law of two twins $(\mathbf{S}_1^-|\mathbf{n}'|\mathbf{S}_3^+)$ and $(\mathbf{S}_3^+|\mathbf{n}'|\mathbf{S}_1^-)$ with the same equally deformed plane p' is expressed by the group

$$T_{1^-3^+}(\mathbf{n}') = m_z = T_{3^-1^+}(\mathbf{n}'), \tag{3.4.3.71}$$

which is different from the $T_{1+3^-}(\mathbf{n})$ of the twin $(\mathbf{S}_1^+|\mathbf{n}|\mathbf{S}_3^-)$.

Representative domain pairs of all orbits of ferroelastic domain pairs (Litvin & Janovec, 1999) are listed in two tables. Table 3.4.3.6 contains representative domain pairs for which compatible domain walls exist and Table 3.4.3.7 lists ferroelastic domain pairs where compatible coexistence of domain states is not possible. Table 3.4.3.6 contains, beside other data, for each ferroelastic domain pair the orientation of two equally deformed planes and the corresponding symmetries of the corresponding four twins which express two twin laws.

3.4.3.6.4. *Ferroelastic domain pairs with compatible domain walls, synoptic table*

As we have seen, for each ferroelastic domain pair for which condition (3.4.3.54) for the existence of coherent domain walls is fulfilled, there exist two perpendicular equally deformed planes. On each of these planes two ferroelastic twins can be formed; these two twins are in a simple relation (one is a reversed twin of the other), have the same symmetry, and can therefore be represented by one of these twins. Then we can say that from one ferroelastic domain pair two different twins can be formed. Each of these twins represents a different 'twin law' that has arisen from the initial domain pair. All four ferroelastic twins can be described in terms of mechanical twinning with the same value of the shear angle ω.

Table 3.4.3.6. *Ferroelastic domain pairs and twins with compatible domain walls*

F_1: symmetry of domain state $\mathbf{S}_1$; g_{1j}: switching operation, $g_{1j}\mathbf{S}_1 = \mathbf{S}_j$; $K(F_1, g_{1j})$: twinning group, group extension of F_1 by g_{1j}; Axis **h**: intersection of compatible walls; Equation: component B expressed as a function of strain components or lattice parameters (see end of table); Wall normals: coordinates of normals $\mathbf{n}_1$ and $\mathbf{n}_2$ of two perpendicular compatible walls, subscript e: wall is charged (see Explanation); ω: obliquity, for numbers (n) see end of table; $\overline{\mathsf{J}}_{1j}$: extended layer-group symmetry of the twin and the wall; $\underline{t}_{1j}^\star$: non-trivial twinning operation of the twin; T_{1j}: layer-group symmetry of the twin and the wall, twin law of the ferroelastic twin; Classification: classification of the twin and the wall (see Table 3.4.4.3).

F_1	g_{1j}	$K(F_1, g_{1j})$	Axis **h**	Equation	Wall normals **n**	ω	$\overline{\mathsf{J}}_{1j}$	$\underline{t}_{1j}^\star$	T_{1j}	Classification
1	$2_z^\star$	$2_z^\star$	$[B\bar{1}0]$	(*a*)	[001] $[1B0]_e$	(1)	$2_z^\star$ $\underline{2}_z^\star$	$\underline{2}_z^\star$	1 $\underline{2}_z^\star$	AR* SI
1	$m_z^\star$	$m_z^\star$	$[B\bar{1}0]$	(*a*)	$[001]_e$ $[1B0]$	(1)	$\underline{m}_z^\star$ $m_z^\star$	$\underline{m}_z^\star$	$\underline{m}_z^\star$ 1	SI AR*
$\bar{1}$	$m_z^\star, 2_z^\star$	$2_z^\star/m_z^\star$	$[B\bar{1}0]$	(*a*)	[001] $[1B0]$	(1)	$2_z^\star/\underline{m}_z^\star$ $\underline{2}_z^\star/m_z^\star$	$\underline{m}_z^\star$ $\underline{2}_z^\star$	$\underline{m}_z^\star$ $\underline{2}_z^\star$	SR SR
2_z	$2_x^\star, 2_y^\star$	$2_x^\star 2_y^\star 2_z$	[001]		[100] [010]	(2)	$2_x^\star\underline{2}_y^\star\underline{2}_z$ $\underline{2}_x^\star 2_y^\star\underline{2}_z$	$\underline{2}_y^\star$ $\underline{2}_x^\star$	$\underline{2}_y^\star$ $\underline{2}_x^\star$	SR SR
2_z	$m_x^\star, m_y^\star$	$m_x^\star m_y^\star 2_z$	[001]		[100] [010]	(2)	$\underline{m}_x^\star m_y^\star\underline{2}_z$ $m_x^\star\underline{m}_y^\star\underline{2}_z$	$\underline{m}_x^\star$ $\underline{m}_y^\star$	$\underline{m}_x^\star$ $\underline{m}_y^\star$	SR SR
2_z	$4_z^\star, 4_z^{3\star}$	$4_z^\star$	[001]	(*b*)	[[1*B*0] [*B*$\bar{1}$0]	(3)	$\underline{2}_z$ $\underline{2}_z$		1 1	AR A$\underline{\mathrm{R}}$
2_z	$\bar{4}_z^\star, \bar{4}_z^{*3}$	$\bar{4}_z^\star$	[001]	(*b*)	[[1*B*0] [*B*$\bar{1}$0]	(3)	$\underline{2}_z$ $\underline{2}_z$		1 1	AR A$\underline{\mathrm{R}}$
2_z	$3_z, 6_z^5$	6_z	[001]	(*c*)	[1*B*0] [*B*$\bar{1}$0]	(4)	$\underline{2}_z$ $\underline{2}_z$		1 1	AR A$\underline{\mathrm{R}}$
	$3_z^2, 6_z$	6_z	[001]	(*c*)	[1*B*0] [*B*$\bar{1}$0]	(4)	$\underline{2}_z$ $\underline{2}_z$		1 1	AR A$\underline{\mathrm{R}}$
2_z	$\bar{3}_z^5, \bar{6}_z$	$6_z/m_z$	[001]	(*c*)	[1*B*0] [*B*$\bar{1}$0]	(4)	$\underline{2}_z$ $\underline{2}_z$		1 1	AR A$\underline{\mathrm{R}}$
	$\bar{3}_z, \bar{6}_z^5$	$6_z/m_z$	[001]	(*c*)	[1*B*0] [*B*$\bar{1}$0]	(4)	$\underline{2}_z$ $\underline{2}_z$		1 1	AR A$\underline{\mathrm{R}}$
2_x	$2_{xy}^\star, 4_z$	$4_z 2_x 2_{xy}$	[*B*$\bar{B}$2]	(*d*)	[110] $[1\bar{1}B]_e$	(5)	$2_{xy}^\star$ $\underline{2}_{xy}^\star$	$\underline{2}_{xy}^\star$	1 $\underline{2}_{xy}^\star$	AR* SI
2_x	$m_{xy}^\star, \bar{4}_z$	$\bar{4}_z 2_x m_{xy}$	[*B*$\bar{B}$2]	(*d*)	$[110]_e$ $[1\bar{1}B]$	(5)	$\underline{m}_{xy}^\star$ $m_{xy}^\star$	$\underline{m}_{xy}^\star$	$\underline{m}_{xy}^\star$ 1	SI AR*
2_x	$2_{x'}^\star, 3_z^2$	$3_z 2_x$	$[\sqrt{3}B, B, \bar{4}]$	(*e*)	$[\bar{1}\sqrt{3}0]$ $[\sqrt{3}1B]_e$	(6)	$2_{x'}^\star$ $\underline{2}_{x'}^\star$	$\underline{2}_{x'}^\star$	1 $\underline{2}_{x'}^\star$	AR* SI

Table 3.4.3.6 (*cont.*)

F_1	g_{1j}	$K(F_1, g_{1j})$	Axis **h**	Equation	Wall normals **n**	ω	$\bar{\mathsf{J}}_{1j}$	$\underline{t}^{\star}_{1j}$	T_{1j}	Classification
2_x	$m^{\star}_{x'}, \bar{3}^5_z$	$\bar{3}_z m_x$	$[\sqrt{3}B, B, \bar{4}]$	(e)	$[\bar{1}\sqrt{30}]_e$ $[\sqrt{3}1B]$	(6)	$\underline{m}^{\star}_{x'}$ $m^{\star}_{x'}$	$\underline{m}^{\star}_{x'}$	$\underline{m}^{\star}_{x'}$ 1	SI AR*
2_x	$2^{\star}_{y'}, 6_z$	$6_z 2_x 2_y$	$[\bar{B}, \sqrt{3}B, \bar{4}]$	(f)	$[\sqrt{3}10]$ $[\bar{1}\sqrt{3}B]_e$	(7)	$2^{\star}_{y'}$ $\underline{2}^{\star}_{y'}$	$\underline{2}^{\star}_{y'}$	1 $\underline{2}^{\star}_{y'}$	AR* SI
2_x	$m^{\star}_{y'}, \bar{6}_z$	$\bar{6}_z 2_x m_y$	$[\bar{B}, \sqrt{3}B, \bar{4}]$	(f)	$[\sqrt{3}10]_e$ $[\bar{1}\sqrt{3}B]$	(7)	$\underline{m}^{\star}_{y'}$ $m^{\star}_{y'}$	$\underline{m}^{\star}_{y'}$	$\underline{m}^{\star}_{y'}$ 1	SI AR*
2_{xy}	$m^{\star}_x, \bar{4}^3_z$	$\bar{4}_z m_x 2_{xy}$	$[0B\bar{1}]$	(g)	$[100]_e$ $[01B]$	(8)	$\underline{m}^{\star}_x$ $m^{\star}_x$	$\underline{m}^{\star}_x$	$\underline{m}^{\star}_x$ 1	SI AR*
m_z	$m^{\star}_x, 2^{\star}_y$	$m^{\star}_x 2^{\star}_y m_z$	$[001]$		$[100]_e$ $[010]$	(2)	$\underline{m}^{\star}_x \underline{2}^{\star}_y m_z$ $m^{\star}_x 2^{\star}_y m_z$	$\underline{m}^{\star}_x$	$\underline{m}^{\star}_x \underline{2}^{\star}_y m_z$ m_z	SI AR*
m_z	$4_z, \bar{4}^3_z$	$4_z/m_z$	$[001]$	(b)	$[1B0]_{e0}$ $[B\bar{1}0]_{0e}$	(3)	m_z m_z		m_z m_z	AI AI
	$4^3_z, \bar{4}_z$	$4_z/m_z$	$[001]$	(b)	$[1B0]_{e0}$ $[B\bar{1}0]_{0e}$	(3)	m_z m_z		m_z m_z	AI AI
m_z	$3_z, \bar{6}^5_z$	$\bar{6}_z$	$[001]$	(c)	$[1B0]_{e0}$ $[B\bar{1}0]_{0e}$	(4)	m_z m_z		m_z m_z	AI AI
	$3^2_z, \bar{6}_z$	$\bar{6}_z$	$[001]$	(c)	$[1B0]_{e0}$ $[B\bar{1}0]_{0e}$	(4)	m_z m_z		m_z m_z	AI AI
m_z	$\bar{3}_z, 6^5_z$	$6_z/m_z$	$[001]$	(c)	$[1B0]_{e0}$ $[B\bar{1}0]_{0e}$	(4)	m_z m_z		m_z m_z	AI AI
	$\bar{3}^5_z, 6_z$	$6_z/m_z$	$[001]$	(c)	$[1B0]_{e0}$ $[B\bar{1}0]_{0e}$	(4)	m_z m_z		m_z m_z	AI AI
m_x	$m^{\star}_{xy}, 4_z$	$4_z m_x m_{xy}$	$[\bar{B}B2]$	(d)	$[110]_e$ $[1\bar{1}B]$	(5)	$\underline{m}^{\star}_{xy}$ $m^{\star}_{xy}$	$\underline{m}^{\star}_{xy}$	$\underline{m}^{\star}_{xy}$ 1	SI AR*
m_x	$2^{\star}_{xy}, \bar{4}_z$	$\bar{4}_z m_x 2_{xy}$	$[\bar{B}B2]$	(d)	$[110]$ $[1\bar{1}B]_e$	(5)	$2^{\star}_{xy}$ $\underline{2}^{\star}_{xy}$	$\underline{2}^{\star}_{xy}$	1 $\underline{2}^{\star}_{xy}$	AR* SI
m_x	$m^{\star}_{x'}, 3^2_z$	$3_z m_x$	$[\sqrt{3}B, B, \bar{4}]$	(e)	$[\bar{1}\sqrt{30}]_e$ $[\sqrt{3}1B]$	(6)	$\underline{m}^{\star}_{x'}$ $m^{\star}_{x'}$	$\underline{m}^{\star}_{x'}$	$\underline{m}^{\star}_{x'}$ 1	SI AR*
m_x	$2^{\star}_{x'}, \bar{3}^5_z$	$\bar{3}_z m_x$	$[\sqrt{3}B, B, \bar{4}]$	(e)	$[\bar{1}\sqrt{30}]$ $[\sqrt{3}1B]_e$	(6)	$2^{\star}_{x'}$ $\underline{2}^{\star}_{x'}$	$\underline{2}^{\star}_{x'}$	1 $\underline{2}^{\star}_{x'}$	AR* SI
m_x	$m^{\star}_{y'}, 6_z$	$6_z m_x m_y$	$[\bar{B}, \sqrt{3}B, \bar{4}]$	(f)	$[\sqrt{3}10]_e$ $[\bar{1}\sqrt{3}B]$	(6)	$\underline{m}^{\star}_{y'}$ $m^{\star}_{y'}$	$\underline{m}^{\star}_{y'}$	$\underline{m}^{\star}_{y'}$ 1	SI AR*
m_x	$2^{\star}_{y'}, \bar{6}_z$	$\bar{6}_z m_x 2_y$	$[\bar{B}, \sqrt{3}B, \bar{4}]$	(f)	$[\sqrt{3}10]$ $[\bar{1}\sqrt{3}B]_e$	(6)	$2^{\star}_{y'}$ $\underline{2}^{\star}_{y'}$	$\underline{2}^{\star}_{y'}$	1 $\underline{2}^{\star}_{y'}$	AR* SI
m_{xy}	$2^{\star}_x, \bar{4}^3_z$	$\bar{4}_z 2_x m_{xy}$	$[0B\bar{1}]$	(h)	$[100]$ $[01B]_e$	(9)	$2^{\star}_x$ $\underline{2}^{\star}_x$	$\underline{2}^{\star}_x$	1 $\underline{2}^{\star}_x$	AR* SI
$2_z/m_z$	$m^{\star}_x, m^{\star}_y$	$m^{\star}_x m^{\star}_y m_z$	$[001]$		$[100]$ $[010]$	(2)	$\underline{m}^{\star}_x m^{\star}_y m_z$ $m^{\star}_x \underline{m}^{\star}_y m_z$	$\underline{m}^{\star}_x$ $\underline{m}^{\star}_y$	$\underline{m}^{\star}_x \underline{2}^{\star}_y m_z$ $\underline{2}^{\star}_x \underline{m}^{\star}_y m_z$	SR SR
$2_z/m_z$	$4^{\star}_z, 4^{3\star}_z$	$4^{\star}_z/m_z$	$[001]$	(b)	$[1B0]$ $[B\bar{1}0]$	(3)	$\underline{2}_z/m_z$ $\underline{2}_z/m_z$		m_z m_z	AR A$\overline{\mathrm{R}}$
$2_z/m_z$	$3_z, 6^5_z$	$6_z/m_z$	$[001]$	(c)	$[1B0]$ $[B\bar{1}0]$	(4)	$\underline{2}_z/m_z$ $\underline{2}_z/m_z$		m_z m_z	AR A$\overline{\mathrm{R}}$
	$3^2_z, 6_z$	$6_z/m_z$	$[001]$	(c)	$[1B0]$ $[B\bar{1}0]$	(4)	$\underline{2}_z/m_z$ $\underline{2}_z/m_z$		m_z m_z	AR A$\overline{\mathrm{R}}$
$2_x/m_x$	$m^{\star}_{xy}, 4_z$	$4_z/m_z m_x m_{xy}$	$[\bar{B}B2]$	(d)	$[110]$ $[1\bar{1}B]$	(5)	$2^{\star}_{xy}/\underline{m}^{\star}_{xy}$ $\underline{2}^{\star}_{xy}/m^{\star}_{xy}$	$\underline{m}^{\star}_{xy}$ $\underline{2}^{\star}_{xy}$	$\underline{m}^{\star}_{xy}$ $\underline{2}^{\star}_{xy}$	SR SR
$2_x/m_x$	$m^{\star}_{x'}, 3^2_z$	$\bar{3}_z m_x$	$[\sqrt{3}B, B, \bar{4}]$	(e)	$[\bar{1}\sqrt{30}]$ $[\sqrt{3}1B]$	(6)	$2^{\star}_{x'}/\underline{m}^{\star}_{x'}$ $\underline{2}^{\star}_{x'}/m^{\star}_{x'}$	$\underline{m}^{\star}_{x'}$ $\underline{2}^{\star}_{x'}$	$\underline{m}^{\star}_{x'}$ $\underline{2}^{\star}_{x'}$	SR SR
$2_x/m_x$	$m^{\star}_{y'}, 6_z$	$6_z/m_z m_x m_y$	$[\bar{B}, \sqrt{3}B, \bar{4}]$	(f)	$[\sqrt{3}10]$ $[\bar{1}\sqrt{3}B]$	(6)	$2^{\star}_{y'}/\underline{m}^{\star}_{y'}$ $\underline{2}^{\star}_{y'}/m^{\star}_{y'}$	$\underline{m}^{\star}_{y'}$ $\underline{2}^{\star}_{y'}$	$\underline{m}^{\star}_{y'}$ $\underline{2}^{\star}_{y'}$	SR SR
$2_x 2_y 2_z$	$2^{\star}_{x\bar{y}}, 2^{\star}_{xy}$	$4^{\star}_z 2_x 2^{\star}_{xy}$	$[001]$		$[110]$ $[1\bar{1}0]$	(11)	$2^{\star}_{xy} \underline{2}^{\star}_{x\bar{y}} \underline{2}_z$ $\underline{2}^{\star}_{xy} 2^{\star}_{x\bar{y}} \underline{2}_z$	$\underline{2}^{\star}_{x\bar{y}}$ $\underline{2}^{\star}_{xy}$	$\underline{2}^{\star}_{x\bar{y}}$ $\underline{2}^{\star}_{xy}$	SR SR
$2_x 2_y 2_z$	$m^{\star}_{x\bar{y}}, m^{\star}_{xy}$	$\bar{4}^{\star}_z 2_x m^{\star}_{xy}$	$[001]$		$[110]$ $[1\bar{1}0]$	(11)	$\underline{m}^{\star}_{xy} m^{\star}_{x\bar{y}} \underline{2}_z$ $m^{\star}_{xy} \underline{m}^{\star}_{x\bar{y}} \underline{2}_z$	$\underline{m}^{\star}_{xy}$ $\underline{m}^{\star}_{x\bar{y}}$	$\underline{m}^{\star}_{xy}$ $\underline{m}^{\star}_{x\bar{y}}$	SR SR
$2_x 2_y 2_z$	$2^{\star}_{x'}, 2^{\star}_{y'}$	$6_z 2_x 2_y$	$[001]$		$[\bar{1}\sqrt{30}]$ $[\sqrt{3}10]$	(10)	$2^{\star}_{x'} \underline{2}^{\star}_{y'} \underline{2}_z$ $\underline{2}^{\star}_{x'} 2^{\star}_{y'} \underline{2}_z$	$\underline{2}^{\star}_{y'}$ $\underline{2}^{\star}_{x'}$	$\underline{2}^{\star}_{y'}$ $\underline{2}^{\star}_{x'}$	SR SR
$2_x 2_y 2_z$	$m^{\star}_{x'}, m^{\star}_{y'}$	$6_z/m_z m_x m_y$	$[001]$		$[\bar{1}\sqrt{30}]$ $[\sqrt{3}10]$	(10)	$\underline{m}^{\star}_{x'} m^{\star}_{y'} \underline{2}_z$ $m^{\star}_{x'} \underline{m}^{\star}_{y'} \underline{2}_z$	$\underline{m}^{\star}_{x'}$ $\underline{m}^{\star}_{y'}$	$\underline{m}^{\star}_{x'}$ $\underline{m}^{\star}_{y'}$	SR SR
$2_{x\bar{y}} 2_{xy} 2_z$	$m^{\star}_x, m^{\star}_y$	$\bar{4}^{\star}_z m_x 2^{\star}_{xy}$	$[001]$		$[100]$ $[010]$	(13)	$\underline{m}^{\star}_x m^{\star}_y \underline{2}_z$ $m^{\star}_x \underline{m}^{\star}_y \underline{2}_z$	$\underline{m}^{\star}_x$ $\underline{m}^{\star}_y$	$\underline{m}^{\star}_x$ $\underline{m}^{\star}_y$	SR SR
$2_{x\bar{y}} 2_{xy} 2_z$	$2^{\star}_{xz}, 4_y$	$4_z 3_p 2_{xy}$	$[B2\bar{B}]$	(k)	$[101]$ $[\bar{1}B1]$	(12)	$2^{\star}_{xz}$ $\underline{2}^{\star}_{xz}$	$\underline{2}^{\star}_{xz}$	1 $\underline{2}^{\star}_{xz}$	AR* SI
$2_{x\bar{y}} 2_{xy} 2_z$	$m^{\star}_{xz}, \bar{4}_y$	$m_z \bar{3}_p m_{xy}$	$[B2\bar{B}]$	(k)	$[101]$ $[\bar{1}B1]$	(12)	$\underline{m}^{\star}_{xz}$ $m^{\star}_{xz}$	$\underline{m}^{\star}_{xz}$	$\underline{m}^{\star}_{xz}$ 1	SI AR*

Table 3.4.3.6 (*cont.*)

F_1	g_{1j}	$K(F_1, g_{1j})$	Axis **h**	Equation	Wall normals **n**	ω	$\bar{\mathsf{J}}_{1j}$	$\underline{t}^{\star}_{1j}$	T_{1j}	Classification
$m_x m_y 2_z$	$m^{\star}_{x\bar{y}}, m^{\star}_{xy}$	$4^{\star}_z m_x m^{\star}_{xy}$	[001]		[110] [1$\bar{1}$0]	(11)	$m^{\star}_{x\bar{y}} \underline{m}^{\star}_{xy} \underline{2}_z$ $\underline{m}^{\star}_{x\bar{y}} m^{\star}_{xy} \underline{2}_z$	$\underline{m}^{\star}_{xy}$ $\underline{m}^{\star}_{x\bar{y}}$	$\underline{m}^{\star}_{xy}$ $\underline{m}^{\star}_{x\bar{y}}$	SR SR
$m_x m_y 2_z$	$2^{\star}_{x\bar{y}}, 2^{\star}_{xy}$	$\bar{4}^{\star}_z m_x 2^{\star}_{xy}$	[001]		[110] [1$\bar{1}$0]	(11)	$2^{\star}_{xy} \underline{2}^{\star}_{x\bar{y}} \underline{2}_z$ $\underline{2}^{\star}_{xy} 2^{\star}_{x\bar{y}} \underline{2}_z$	$\underline{2}^{\star}_{x\bar{y}}$ $\underline{2}^{\star}_{xy}$	$\underline{2}^{\star}_{x\bar{y}}$ $\underline{2}^{\star}_{xy}$	SR SR
$m_x m_y 2_z$	$m^{\star}_{x'}, m^{\star}_{y'}$	$6_z m_x m_y$	[001]		[$\bar{1}\sqrt{30}$] [$\sqrt{3}$10]	(10)	$\underline{m}^{\star}_{x'} m^{\star}_{y'} \underline{2}_z$ $m^{\star}_{x'} \underline{m}^{\star}_{y'} \underline{2}_z$	$\underline{m}^{\star}_{x'}$ $\underline{m}^{\star}_{y'}$	$\underline{m}^{\star}_{x'}$ $\underline{m}^{\star}_{y'}$	SR SR
$m_x m_y 2_z$	$2^{\star}_{x'}, 2^{\star}_{y'}$	$6_z / m_z m_x m_y$	[001]		[$\bar{1}\sqrt{30}$] [$\sqrt{3}$10]	(10)	$2^{\star}_{x'} \underline{2}^{\star}_{y'} \underline{2}_z$ $\underline{2}^{\star}_{x'} 2^{\star}_{y'} \underline{2}_z$	$\underline{2}^{\star}_{y'}$ $\underline{2}^{\star}_{x'}$	$\underline{2}^{\star}_{y'}$ $\underline{2}^{\star}_{x'}$	SR SR
$m_x 2_y m_z$	$m^{\star}_{x'}, 2^{\star}_{y'}$	$\bar{6}_z m_x 2_y$	[001]		[$\bar{1}\sqrt{30}$]$_e$ [$\sqrt{3}$10]	(10)	$\underline{m}^{\star}_{x'} \underline{2}^{\star}_{y'} m_z$ $m^{\star}_{x'} 2^{\star}_{y'} m_z$	$\underline{m}^{\star}_{x'}$	$\underline{m}^{\star}_{x'} \underline{2}^{\star}_{y'} m_z$ m_z	SI AR*
$2_x m_y m_z$	$m^{\star}_{x\bar{y}}, 2^{\star}_{xy}$	$4_z / m_z m_x m_{xy}$	[001]		[110] [1$\bar{1}$0]$_e$	(11)	$2^{\star}_{xy} m^{\star}_{x\bar{y}} m_z$ $\underline{2}^{\star}_{xy} \underline{m}^{\star}_{x\bar{y}} m_z$	$\underline{m}^{\star}_{x\bar{y}}$	m_z $\underline{2}^{\star}_{xy} \underline{m}^{\star}_{x\bar{y}} m_z$	AR* SI
$2_x m_y m_z$	$m^{\star}_{y'}, 2^{\star}_{x'}$	$\bar{6}_z 2_x m_y$	[001]		[$\bar{1}\sqrt{30}$] [$\sqrt{3}$10]$_e$	(10)	$2^{\star}_{x'} m^{\star}_{y'} m_z$ $\underline{2}^{\star}_{x'} \underline{m}^{\star}_{y'} m_z$	$\underline{m}_{y'}$	m_z $\underline{2}^{\star}_{x'} \underline{m}^{\star}_{y'} m_z$	AR* SI
$2_x m_y m_z$	$m^{\star}_{x'}, 2^{\star}_{y'}$	$6_z / m_z m_x m_y$	[001]		[$\bar{1}\sqrt{30}$]$_e$ [$\sqrt{3}$10]	(10)	$\underline{m}^{\star}_{x'} \underline{2}^{\star}_{y'} m_z$ $m^{\star}_{x'} 2^{\star}_{y'} m_z$	$\underline{m}^{\star}_{x'}$	$\underline{m}^{\star}_{x'} \underline{2}^{\star}_{y'} m_z$ m_z	SI AR*
$m_{x\bar{y}} m_{xy} 2_z$	$2^{\star}_x, 2^{\star}_y$	$\bar{4}^{\star}_z 2^{\star}_x m_{xy}$	[001]		[100] [010]	(13)	$2^{\star}_x \underline{2}^{\star}_y \underline{2}_z$ $\underline{2}^{\star}_x 2^{\star}_y \underline{2}_z$	$\underline{2}^{\star}_y$ $\underline{2}^{\star}_x$	$\underline{2}^{\star}_y$ $\underline{2}^{\star}_x$	SR SR
$m_{x\bar{y}} m_{xy} 2_z$	$m^{\star}_{xz}, \bar{4}_y$	$\bar{4}_z 3_p m_{xy}$	[$B2\bar{B}$]	(k)	[101]$_e$ [$\bar{1}B1$]	(12)	$\underline{m}^{\star}_{xz}$ $m^{\star}_{xz}$	$\underline{m}^{\star}_{xz}$	$\underline{m}^{\star}_{xz}$ 1	SI AR*
$m_{x\bar{y}} m_{xy} 2_z$	$2^{\star}_{xz}, 4_y$	$m_z \bar{3}_p m_{xy}$	[$B2\bar{B}$]	(k)	[101] [$\bar{1}B1$]$_e$	(12)	$2^{\star}_{xz}$ $\underline{2}^{\star}_{xz}$	$\underline{2}^{\star}_{xz}$	1 $\underline{2}^{\star}_{xz}$	AR* SI
$m_{x\bar{y}} 2_{xy} m_z$	$m^{\star}_{xz}, 4_y$	$m_z \bar{3}_p m_{xy}(m^{\star}_{xz})$	[$B2\bar{B}$]	(k)	[101]$_e$ [$\bar{1}B1$]	(12)	$\underline{m}^{\star}_{xz}$ $m^{\star}_{xz}$	$\underline{m}^{\star}_{xz}$	$\underline{m}^{\star}_{xz}$ 1	SI AR*
$m_{x\bar{y}} 2_{xy} m_z$	$2^{\star}_{xz}, \bar{4}_y$	$m_z \bar{3}_p m_{xy}(2^{\star}_{xz})$	[$B2\bar{B}$]	(k)	[101] [$\bar{1}B1$]$_e$	(12)	$2^{\star}_{xz}$ $\underline{2}^{\star}_{xz}$	$\underline{2}^{\star}_{xz}$	1 $\underline{2}^{\star}_{xz}$	AR* SI
$m_x m_y m_z$	$m^{\star}_{xy}, m^{\star}_{x\bar{y}}$	$4^{\star}_z / m_z m_x m^{\star}_{xy}$	[001]		[110] [1$\bar{1}$0]	(10)	$m^{\star}_{x\bar{y}} \underline{m}^{\star}_{xy} m_z$ $\underline{m}^{\star}_{x\bar{y}} m^{\star}_{xy} m_z$	$\underline{m}^{\star}_{xy}$ $\underline{m}^{\star}_{x\bar{y}}$	$\underline{2}^{\star}_{x\bar{y}} \underline{m}^{\star}_{xy} m_z$ $\underline{m}^{\star}_{x\bar{y}} 2^{\star}_{xy} m_z$	SR SR
$m_x m_y m_z$	$m^{\star}_{x'}, m^{\star}_{y'}$	$6_z / m_z m_x m_y$	[001]		[$\bar{1}\sqrt{30}$] [$\sqrt{3}$10]	(10)	$\underline{m}^{\star}_{x'} m^{\star}_{y'} m_z$ $m^{\star}_{x'} \underline{m}^{\star}_{y'} m_z$	$\underline{m}^{\star}_{x'}$ $\underline{m}^{\star}_{y'}$	$\underline{m}^{\star}_{x'} \underline{2}^{\star}_{y'} m_z$ $\underline{2}^{\star}_{x'} \underline{m}^{\star}_{y'} m_z$	SR SR
$m_{xy} m_{\bar{x}y} m_z$	$m^{\star}_{xz}, 4_y$	$m_z \bar{3}_p m_{xy}$	[$B2\bar{B}$]	(k)	[101] [$\bar{1}B1$]	(12)	$2^{\star}_{xz} / \underline{m}^{\star}_{xz}$ $\underline{2}^{\star}_{xz} / m^{\star}_{xz}$	$\underline{m}^{\star}_{xz}$ $\underline{2}^{\star}_{xz}$	$\underline{m}^{\star}_{xz}$ $\underline{2}^{\star}_{xz}$	SR SR
4_z	$2^{\star}_{xz}, 4_y$	$4_z 3_p 2_{xy}$	[010]		[101] [$\bar{1}$01]$_e$	(14)	$2^{\star}_{xz}$ $\underline{2}^{\star}_{xz}$	$\underline{2}^{\star}_{xz}$	1 $\underline{2}^{\star}_{xz}$	AR* SI
4_z	$m^{\star}_{xz}, \bar{4}_y$	$m_z \bar{3}_p m_{xy}$	[010]		[101]$_e$ [$\bar{1}$01]	(14)	$\underline{m}^{\star}_{xz}$ $m^{\star}_{xz}$	$\underline{m}^{\star}_{xz}$	$\underline{m}^{\star}_{xz}$ 1	SI AR*
$\bar{4}_z$	$m^{\star}_{xz}, \bar{4}_y$	$\bar{4}_z 3_p m_{xy}$	[010]		[101] [$\bar{1}$01]	(14)	$\underline{m}^{\star}_{xz}$ $m^{\star}_{xz}$	$\underline{m}^{\star}_{xz}$	$\underline{m}^{\star}_{xz}$ 1	SI AR*
$\bar{4}_z$	$2^{\star}_{xz}, 4_y$	$m_z \bar{3}_p m_{xy}$	[010]		[101] [$\bar{1}$01]$_e$	(14)	$2^{\star}_{xz}$ $\underline{2}^{\star}_{xz}$	$\underline{2}^{\star}_{xz}$	1 $\underline{2}^{\star}_{xz}$	AR* SI
$4_z / m_z$	$m^{\star}_{xz}, 4_y$	$m_z \bar{3}_p m_{xy}$	[010]		[101] [$\bar{1}$01]	(14)	$2^{\star}_{xz} / \underline{m}^{\star}_{xz}$ $\underline{2}^{\star}_{xz} / m^{\star}_{xz}$	$\underline{m}^{\star}_{xz}$ $\underline{2}^{\star}_{xz}$	$\underline{m}^{\star}_{xz}$ $\underline{2}^{\star}_{xz}$	SR SR
$4_z 2_x 2_{xy}$	$2^{\star}_{xz}, 2^{\star}_{x\bar{z}}$	$4_z 3_p 2_{xy}$	[010]		[101] [$\bar{1}$01]	(14)	$2^{\star}_{xz} \underline{2}^{\star}_{x\bar{z}} \underline{2}_y$ $\underline{2}^{\star}_{xz} 2^{\star}_{x\bar{z}} \underline{2}_y$	$\underline{2}^{\star}_{x\bar{z}}$ $\underline{2}^{\star}_{xz}$	$\underline{2}^{\star}_{x\bar{z}}$ $\underline{2}^{\star}_{xz}$	SR SR
$4_z 2_x 2_{xy}$	$m^{\star}_{xz}, m^{\star}_{x\bar{z}}$	$m_z \bar{3}_p m_{xy}$	[010]		[101] [$\bar{1}$01]	(14)	$\underline{m}^{\star}_{xz} m^{\star}_{x\bar{z}} \underline{2}_y$ $m^{\star}_{xz} \underline{m}^{\star}_{x\bar{z}} \underline{2}_y$	$\underline{m}^{\star}_{xz}$ $\underline{m}^{\star}_{x\bar{z}}$	$\underline{m}^{\star}_{xz}$ $\underline{m}^{\star}_{x\bar{z}}$	SR SR
$4_z m_x m_{xy}$	$m^{\star}_{x\bar{z}}, 2^{\star}_{xz}$	$m_z \bar{3}_p m_{xy}$	[010]		[101] [$\bar{1}$01]$_e$	(14)	$2^{\star}_{xz} m^{\star}_{x\bar{z}} m_y$ $\underline{2}^{\star}_{xz} \underline{m}^{\star}_{x\bar{z}} m_y$	$\underline{2}^{\star}_{xz}$	m_y $\underline{2}^{\star}_{xz} \underline{m}^{\star}_{x\bar{z}} m_y$	AR* SI
$\bar{4}_z 2_x m_{xy}$	$m^{\star}_{xz}, m^{\star}_{x\bar{z}}$	$\bar{4}_z 3_p m_{xy}$	[010]		[101] [$\bar{1}$01]	(14)	$\underline{m}^{\star}_{xz} m^{\star}_{x\bar{z}} \underline{2}_y$ $m^{\star}_{xz} \underline{m}^{\star}_{x\bar{z}} \underline{2}_y$	$\underline{m}^{\star}_{xz}$ $\underline{m}^{\star}_{x\bar{z}}$	$\underline{m}^{\star}_{xz}$ $\underline{m}^{\star}_{x\bar{z}}$	SR SR
$\bar{4}_z m_x 2_{xy}$	$m^{\star}_{x\bar{z}}, 2^{\star}_{xz}$	$m_z \bar{3}_p m_{xy}$	[010]		[101] [$\bar{1}$01]	(14)	$2^{\star}_{xz} m^{\star}_{x\bar{z}} m_y$ $\underline{2}^{\star}_{xz} \underline{m}^{\star}_{x\bar{z}} m_y$	$\underline{m}^{\star}_{x\bar{z}}$	m_y $\underline{2}^{\star}_{xz} \underline{m}^{\star}_{x\bar{z}} m_y$	AR* SR
$\bar{4}_z 2_x m_{xy}$	$2^{\star}_{xz}, 2^{\star}_{x\bar{z}}$	$m_z \bar{3}_p m_{xy}$	[010]		[101] [$\bar{1}$01]	(14)	$2^{\star}_{xz} 2^{\star}_{x\bar{z}} 2_y$ $\underline{2}^{\star}_{xz} \underline{2}^{\star}_{x\bar{z}} 2_y$	$\underline{2}^{\star}_{x\bar{z}}$ $\underline{2}^{\star}_{x\bar{z}}$	$\underline{2}^{\star}_{x\bar{z}}$ $\underline{2}^{\star}_{xz} \underline{2}^{\star}_{x\bar{z}} 2_y$	SR SI
$4_z / m_z m_x m_{xy}$	$m^{\star}_{xz}, m^{\star}_{\bar{x}z}$	$m_z \bar{3}_p m_{xy}$	[010]		[101] [$\bar{1}$01]	(14)	$\underline{m}^{\star}_{xz} m^{\star}_{\bar{x}z} m_y$ $m^{\star}_{xz} \underline{m}^{\star}_{\bar{x}z} m_y$	$\underline{m}^{\star}_{xz}$ $\underline{m}^{\star}_{\bar{x}z}$	$\underline{m}^{\star}_{xz} \underline{2}^{\star}_{\bar{x}z} m_y$ $\underline{2}^{\star}_{xz} \underline{m}^{\star}_{\bar{x}z} m_y$	SR SR
3_p	$2^{\star}_x, 3_r$	$2_z 3_p$	[01$\bar{1}$]		[100] [011]$_e$	(15)	$2^{\star}_x$ $\underline{2}^{\star}_x$	$\underline{2}^{\star}_x$	1 $\underline{2}^{\star}_x$	AR* SI
3_p	$m^{\star}_x, \bar{3}_r$	$m_z \bar{3}_p$	[01$\bar{1}$]		[100]$_e$ [011]	(15)	$\underline{m}^{\star}_x$ $m^{\star}_x$	$\underline{m}^{\star}_x$	$\underline{m}^{\star}_x$ 1	SI AR*
3_p	$2^{\star}_{xy}, 4_y$	$4_z 3_p 2_{xy}$	[1$\bar{1}$0]		[001]$_e$ [110]	(15)	$\underline{2}^{\star}_{xy}$ $2^{\star}_{xy}$	$\underline{2}^{\star}_{xy}$	$\underline{2}^{\star}_{xy}$ 1	SI AR*
3_p	$m^{\star}_{xy}, \bar{4}_y$	$\bar{4}_z 3_p m_{xy}$	[1$\bar{1}$0]		[001] [110]$_e$	(15)	$m^{\star}_{xy}$ $\underline{m}^{\star}_{xy}$	$\underline{m}^{\star}_{xy}$	1 $\underline{m}^{\star}_{xy}$	AR* SI

Table 3.4.3.6 (*cont.*)

F_1	g_{1j}	$K(F_1, g_{1j})$	Axis **h**	Equation	Wall normals **n**	ω	$\bar{\mathsf{J}}_{1j}$	$t^\star_{1j}$	T_{1j}	Classification
$\bar{3}_p$	$m^\star_x, 3_r$	$m_z\bar{3}_p$	$[01\bar{1}]$		[100] [011]	(15)	$2^\star_x/\underline{m}^\star_x$ $\underline{2}^\star_x/m^\star_x$	$\underline{m}^\star_x$ $\underline{2}^\star_x$	$\underline{m}^\star_x$ $\underline{2}^\star_x$	SR SR
$\bar{3}_p$	$m^\star_{xy}, 4_y$	$m_z\bar{3}_p m_{xy}$	$[1\bar{1}0]$		[001] [110]	(15)	$2^\star_{xy}/m^\star_{xy}$ $2^\star_{xy}/\underline{m}^\star_{xy}$	$\underline{2}^\star_{xy}$ $\underline{m}^\star_{xy}$	$\underline{2}^\star_{xy}$ $\underline{m}^\star_{xy}$	SR SR
$3_p2_{x\bar{y}}$	$2^\star_x, 2^\star_{yz}$	$4_z3_p2_{xy}$	$[01\bar{1}]$		[100] [011]	(15)	$2^\star_x\underline{2}^\star_{yz}\underline{2}^\star_{y\bar{z}}$ $\underline{2}^\star_x2^\star_{yz}\underline{2}^\star_{y\bar{z}}$	$\underline{2}^\star_{yz}$ $\underline{2}^\star_x$	$\underline{2}^\star_{yz}$ $\underline{2}^\star_x$	SR SR
$3_p2_{x\bar{y}}$	$m^\star_x, m^\star_{yz}$	$m_z\bar{3}_p m_{xy}$	$[01\bar{1}]$		[100] [011]	(15)	$\underline{m}^\star_x m^\star_{yz}\underline{2}^\star_{y\bar{z}}$ $m^\star_x\underline{m}^\star_{yz}\underline{2}^\star_{y\bar{z}}$	$\underline{m}^\star_x$ $\underline{m}^\star_{yz}$	$\underline{m}^\star_x$ $\underline{m}^\star_{yz}$	SR SR
$3_pm_{x\bar{y}}$	$2^\star_x, m^\star_{yz}$	$\bar{4}_z3_pm_{xy}$	$[01\bar{1}]$		[100] $[011]_e$	(15)	$m^\star_{yz}m_{y\bar{z}}2^\star_x$ $\underline{m}^\star_{yz}m_{y\bar{z}}\underline{2}^\star_x$	 $\underline{m}^\star_{yz}$	$m_{y\bar{z}}$ $\underline{m}^\star_{yz}m_{y\bar{z}}\underline{2}^\star_x$	AR* SI
$3_pm_{x\bar{y}}$	$m^\star_x, 2^\star_{yz}$	$m_z\bar{3}_pm_{xy}$	$[01\bar{1}]$		$[100]_e$ [011]	(15)	$\underline{m}^\star_x\underline{2}^\star_{yz}m_{y\bar{z}}$ $m^\star_x2^\star_{yz}m_{y\bar{z}}$	$\underline{m}^\star_x$	$\underline{m}^\star_x\underline{2}^\star_{yz}m_{y\bar{z}}$ $m_{y\bar{z}}$	SI AR*
$\bar{3}_pm_{x\bar{y}}$	$m^\star_x, m^\star_{yz}$	$m_z\bar{3}_pm_{xy}$	$[01\bar{1}]$		[100] [011]	(15)	$\underline{m}^\star_x m^\star_{yz}m_{y\bar{z}}$ $m^\star_x\underline{m}^\star_{yz}m_{y\bar{z}}$	$\underline{m}^\star_x$ $\underline{m}^\star_{yz}$	$\underline{m}^\star_x\underline{2}^\star_{yz}m_{y\bar{z}}$ $\underline{2}^\star_x\underline{m}^\star_{yz}m_{y\bar{z}}$	SR SR

Expressions for obliquity ω as a function of spontaneous strain components and lattice parameters

Expression	ω as a function of spontaneous strain components $\begin{pmatrix} q & v & u \\ v & r & t \\ u & t & s \end{pmatrix}$	ω as a function of lattice parameters $a, b, c; \alpha = \measuredangle(b; c), \beta = \measuredangle(a; c), \gamma = \measuredangle(a; b)$ 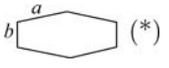
(1)	$\omega = 2\sqrt{t^2 + u^2}$	$\omega = \left\lvert \arccos \dfrac{\sqrt{1 - \cos^2\alpha - \cos^2\beta - \cos^2\gamma + 2\cos\alpha\cos\beta\cos\gamma}}{\sin\gamma} \right\rvert$
(2)	$\omega = 2\lvert v \rvert$	$\omega = \lvert \pi/2 - \gamma \rvert$
(3)	$\omega = \sqrt{(q-r)^2 + 4v^2}$	$\omega = \left\lvert \arcsin \dfrac{\sqrt{(2ab\cos\gamma)^2 + (b^2 - a^2)}}{b^2 - a^2} \right\rvert$
(4)	$\omega = \dfrac{\sqrt{3}}{2}\sqrt{(q-r)^2 + 4v^2}$	$\omega = \lvert \pi/2 - \psi_1 - \psi_2 \rvert$ $\psi_1 = \operatorname{arccotan} \dfrac{c^2(a^2 + b^2 - 2d^2) - (a^2 - b^2)^2 + D(a^2 - b^2 - d^2)}{(D - b^2 + d^2)\sqrt{4a^2d^2 - (a^2 - b^2 - d^2)^2}}$ $\psi_2 = \operatorname{arccotan} \dfrac{b^2(a^2 - b^2) + d^2(a^2 - b^2) - D(a^2 - b^2 + d^2)}{(D - b^2 + d^2)\sqrt{4a^2d^2 - (a^2 - b^2 - d^2)^2}}$ $D = \sqrt{(a^2 - d^2)^2 - (a^2 - b^2)(b^2 - d^2)}$
(5)	$\omega = \sqrt{(q-r)^2 + 2t^2}$	$\omega = \left\lvert \arcsin \dfrac{c^2(a^2 + b^2)\sin^2\alpha - b^2(a + c\cos\alpha)(2Da + c\cos\alpha)}{\sqrt{c^2(a^2 + b^2)\sin^2\alpha + b^2(a + c\cos\alpha)^2}\sqrt{c^2(a^2 + b^2)\sin^2\alpha + b^2(2Da + c\cos\alpha)^2}} \right\rvert$ $D = \dfrac{ac\cos\alpha}{b^2 - a^2}$

Table 3.4.3.6 (*cont.*)

Expression	ω as a function of spontaneous strain components $\begin{pmatrix} q & v & u \\ v & r & t \\ u & t & s \end{pmatrix}$	ω as a function of lattice parameters $a, b, c; \alpha = \angle(b; c), \beta = \angle(a; c), \gamma = \angle(a; b)$ 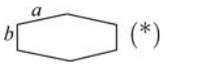 (*)
(6)	$\omega = \dfrac{\sqrt{3}}{2}\sqrt{(q-r)^2 + 4t^2}$	$\omega = \left\lvert \arcsin \dfrac{(4a^2 - b^2)\left[\left(1 - \dfrac{c\cos\beta}{a+b}\right)b\cos\beta - \dfrac{c}{2}\right] + \dfrac{3cb^2\sin^2\beta}{2}}{\sqrt{4a^2 - b^2(1 - 9\sin^2\beta)}\sqrt{(ac\sin\beta)^2 + (4a^2 - b^2)\left[1 - \dfrac{c\cos\beta}{a+b})b - \dfrac{c\cos\beta}{2}\right]^2}} \right\rvert$ (*)
(7)	$\omega = 2\lvert t\rvert$	$\omega = \lvert\pi/2 - \alpha\rvert$
(8)	$\omega = \dfrac{\sqrt{3}}{2}\sqrt{(q-r)^2 + 4t^2}$	$\omega = \left\lvert \arcsin \dfrac{3b^2c - c(4a^2 - b^2)\sin^2\alpha + 2b^2D\sqrt{4a^2 - b^2}\cos\alpha}{\sqrt{b^2 + (4a^2 - b^2)\sin^2\alpha}\sqrt{9b^2c^2 + (4a^2 - b^2)(c^2\sin^2\alpha + 4b^2D^2) + 12b^2Dc\sqrt{4a^2 - b^2}}} \right\rvert$ (*) $D = \dfrac{2ac\cos\alpha}{b^2 - a^2}$
(9)	$\omega = 2\sqrt{q^2 + f^2}$	$\omega = \left\lvert \arccos \dfrac{\sqrt{1 - \cos^2\alpha - \cos^2\beta - \cos^2\gamma + 2\cos\alpha\cos\beta\cos\gamma}}{\sin\alpha} \right\rvert$
(10)	$\omega = \dfrac{\sqrt{3}}{2}\lvert q - r\rvert$	$\omega = \left\lvert \arcsin \dfrac{b^2 - a^2}{a\sqrt{2b^2 + a^2}} \right\rvert$
(11)	$\omega = \lvert q - r\rvert$	$\omega = \left\lvert \arcsin \dfrac{a^2 - b^2}{b^2 + a^2} \right\rvert$
(12)	$\omega = \sqrt{(q-s)^2 + 2v^2}$	$\omega = \left\lvert \arcsin \dfrac{c^2(D\cos\gamma - 1) - a^2\sin^2\gamma}{\sqrt{c^2 + a^2\sin^2\gamma}\sqrt{4c^2(D^2 - D\cos\gamma) + c^2 + a^2\sin^2\gamma}} \right\rvert$ $D = \dfrac{2a^2\cos\gamma}{c^2 - a^2}$
(13)	$\omega = 2\lvert v\rvert$	$\omega = \lvert\pi/2 - \gamma\rvert$
(14)	$\omega = \lvert q - s\rvert$	$\omega = \left\lvert \arcsin \dfrac{a^2 - c^2}{c^2 + a^2} \right\rvert$
(15)	$\omega = 2\sqrt{2}\lvert v\rvert$	$\omega = \left\lvert \arcsin \dfrac{\sqrt{2}\cos\alpha}{1 + \cos\alpha} \right\rvert$

Table 3.4.3.6 (*cont.*)

Expressions for component B of wall normal as a function of spontaneous strain components and lattice parameters

Equation	B as a function of spontaneous strain components $\begin{pmatrix} q & v & u \\ v & r & t \\ u & t & s \end{pmatrix}$	B as a function of lattice parameters $a, b, c; \alpha = \measuredangle(b; c), \beta = \measuredangle(a; c), \gamma = \measuredangle(a; b)$
(*a*)	$B = \dfrac{t}{u}$	
(*b*)	$B = \dfrac{2v + \sqrt{(q-r)^2 + 4v^2}}{q-r}$	$B = \dfrac{-2ab\cos\gamma + \sqrt{(2ab\cos\gamma)^2 + (b^2 - a^2)}}{b^2 - a^2}$
(*c*)	$B = \dfrac{(q-r) + 2\sqrt{3}v + 4\sqrt{(q-r)^2 + 4v^2}}{\sqrt{3}(r-q) + 2v}$	$B = 2\dfrac{a^2 - c^2 - \sqrt{(a^2 - c^2)^2 - (a^2 - b^2)(b^2 - c^2)}}{a^2 - b^2} - 1$
(*d*)	$B = \dfrac{2t}{q-r}$	
(*e*)	$B = \dfrac{4t}{r-q}$	
(*f*)	$B = \dfrac{4t}{q-r}$	
(*g*)	$B = \dfrac{4t}{r-q}$	
(*h*)	$B = \dfrac{-u}{v}$	
(*k*)	$B = \dfrac{2v}{s-v}$	$B = \dfrac{2a^2\cos\gamma}{c^2 - a^2}$

3.4.3.6.4.1. *Explanation of Table 3.4.3.6*

Table 3.4.3.6 presents representative domain pairs of all classes of ferroelastic domain pairs for which compatible domain walls exist. The first five columns concern the domain pair. In subsequent columns, each row splits into two rows describing the orientation of two associated perpendicular equally deformed planes and the symmetry properties of the four domain twins that can be formed from the given domain pair. We explain the meaning of each column in detail.

The first three columns specify *domain pairs*.

F_1: point-group symmetry (stabilizer in K_{1j}) of the first domain state $\mathbf{S}_1$ in a single-domain orientation.

g_{1j}: switching operations (if available) that specify the domain pair $(\mathbf{S}_1, \mathbf{S}_j = g_{1j}\mathbf{S}_1)$. Subscripts x, y, z specify the orientation of the symmetry operations in the Cartesian coordinate system of K_{1j}. Subscripts x', y' and x'', y'' denote a Cartesian coordinate system rotated about the z axis through 120 and 240°, respectively, from the Cartesian coordinate axes x and y. Diagonal directions are abbreviated: $p = [111]$, $q = [\bar{1}\bar{1}1]$, $r = [1\bar{1}\bar{1}]$, $s = [\bar{1}1\bar{1}]$. Where possible, mirror planes and 180° rotations are chosen such that the two perpendicular permissible walls have crystallographic orientations.

K_{1j}: twinning group $K(F_1, g_{1j})$ of the domain pair $(\mathbf{S}_1, \mathbf{S}_j)$. For the pair with $F_1 = m_{x\bar{y}}2_{xy}m_z$ and $K = m\bar{3}m$, where the twinning group does not specify the domain pair unambiguously, we add after K_{1j} in parentheses a switching operation $2^\star_{xz}$ or $m^\star_{xz}$ that defines the domain pair.

Axis: axis of ferroelastic domain pair around which single-domain states must be rotated to establish a contact along a compatible domain wall. This axis is parallel to the intersection of the two compatible domain walls given in the column *Wall normals* and its direction $\mathbf{h}$ is defined by a vector product $\mathbf{h} = \mathbf{n}_1 \times \mathbf{n}_2$ of normal vectors $\mathbf{n}_1$ and $\mathbf{n}_2$ of these walls. The letter B denotes components of $\mathbf{h}$ which depend on spontaneous strain.

Equation: a reference to an expression, given at the end of the table, for the direction $\mathbf{h}$ of the axis, where the component B in the column *Axis* is expressed as functions of spontaneous strain components, and the matrices above these expressions give the form of the 'absolute' spontaneous strain.

Wall normals: orientation of equally deformed planes. As explained above, each plane represents two mutually reversed compatible domain walls. Numbers or parameters B, C given in parentheses can be interpreted either as components of normal vectors to compatible walls or as intercepts analogous to Miller indices: Planes of compatible domain walls $Ax_1 + Bx_2 + Cx_3 = 0$

Table 3.4.3.7. *Ferroelastic domain pairs with no compatible domain walls*

F_1 is the symmetry of $\mathbf{S}_1$, g_{1j} is the switching operation, K_{1j} is the twinning group. Pair is the domain pair type, where ns is non-transposable simple and nm is non-transposable multiple (see Table 3.4.3.2). $v = z$, $p = [111]$, $q = [\bar{1}\bar{1}1]$, $r = [1\bar{1}\bar{1}]$, $s = [\bar{1}1\bar{1}]$ (see Table 3.4.2.5 and Fig. 3.4.2.3).

F_1	g_{1j}	K_{1j}	Pair
1	4_z	4_z	ns
1	$\bar{4}_z$	$\bar{4}_z$	ns
1	3_v	3_v	ns
1	$\bar{3}_v$	$\bar{3}_v$	ns
1	6_z	6_z	ns
1	$\bar{6}_z$	$\bar{6}_z$	ns
$\bar{1}$	4_z, 4_z^3	$4_z/m_z$	ns
$\bar{1}$	3_v, 3_v^2	$\bar{3}_v$	ns
$\bar{1}$	6_z, 6_z^5	$6_z/m_z$	ns
2_z	3_p, 3_p^2	$2_z 3_p$	nm
2_z	$\bar{3}_p$, $\bar{3}_p^5$	$m_z\bar{3}_p$	nm
2_{xy}	3_p, 3_p^2	$4_z 3_p 2_{xy}$	nm
2_{xy}	$\bar{3}_p$, $\bar{3}_p^5$	$m_z\bar{3}_p m_{xy}$	nm
m_z	3_p, 3_p^2	$m_z 3_p^2$	nm
m_{xy}	3_p, 3_p^2	$\bar{4}_z 3_p m_{xy}$	nm
m_{xy}	4_x, 4_x^3	$m_z\bar{3}_p m_{xy}$	nm
$2_z/m_z$	3_p, 3_p^2	$m_z\bar{3}_p$	nm
$2_{xy}/m_{xy}$	3_p, 3_p^2	$m_z\bar{3}_p m_{xy}$	nm
$2_x 2_y 2_z$	3_p, 3_p^2	$2_z 3_p$	ns
$2_x 2_y 2_z$	$\bar{3}_p$, $\bar{3}_p^5$	$m_z\bar{3}_p$	ns
$m_x m_y 2_z$	3_p, 3_p^2	$m_z\bar{3}_p$	nm
$m_x m_y m_z$	3_p, 3_p^2	$m_z\bar{3}_p$	ns

and $A'x_1 + B'x_2 + C'x_3 = 0$ [see equations (3.4.3.55)] pass through the origin of the Cartesian coordinate system of K_{1j} and have normal vectors $\mathbf{n}_1 = [ABC]$ and $\mathbf{n}_2 = [A'B'C']$. It is possible to find a plane with the same normal vector $[ABC]$ but not passing through the origin, *e.g.* $Ax_1 + Bx_2 + Cx_3 = 1$. Then parameters A, B and C can be interpreted as the reciprocal values of the oriented intercepts on the coordinate axes cut by this plane, $[x_1/(1/A)] + [x_2/(1/B)] + [x_3/(1/C)] = 1$. In analogy with Miller indices, the symbol (ABC) is used for expressing the orientation of a wall. However, parameters A, B and C are not Miller indices, since they are expressed in an orthonormal and not a crystallographic coordinate system. A left square bracket [in front of two equally deformed planes signifies that the two domain walls (domain twins) associated with one equally deformed plane are crystallographically equivalent (in K_{1j}) with two domain walls (twins) associated with the perpendicular equally deformed plane, *i.e.* all four compatible domain walls (domain twins) that can be formed from domain pair $(\mathbf{S}_1, \mathbf{S}_j)$ are crystallographically equivalent in K_{1j} (see Fig. 3.4.3.8).

The subscript e indicates that the wall carries a nonzero polarization charge, Div $\mathbf{P} \neq 0$. This can happen in ferroelectric domain pairs with spontaneous polarization not parallel to the axis of the pair. If one domain wall is charged then the perpendicular wall is not charged. In a few cases, polarization and/or orientation of the domain wall is not determined by symmetry; then it is not possible to specify which of the two walls is charged. In such cases, a subscript $e0$ or $0e$ indicates that one of the two walls is charged and the other is not.

ω: reference to an expression, given at the end of the table, in which the shear angle ω (in radians) is given as a function of the 'absolute' spontaneous strain components, defined in a matrix given above the equations.

$\bar{\mathsf{J}}_{1j}$: symmetry of the 'twin pair'. The meaning of this group and its symbol is explained in the next section. This group specifies the symmetry properties of a ferroelastic domain twin and the reversed twin with compatible walls of a given orientation and with domain states $\mathbf{S}_1^+, \mathbf{S}_j^-$ and $\mathbf{S}_1^+, \mathbf{S}_j^-$. This group can be used for designating a twin law of the ferroelastic domain twin.

$\underline{t}_{1j}^{\star}$: one non-trivial twinning operation of the twin $\mathbf{S}_1[ABC]\mathbf{S}_j$ and the wall. An underlined symbol with a star symbol signifies an operation that inverts the wall normal and exchanges the domain states (see the next section).

T_{1j}: layer-group symmetry of the ferroelastic domain twin and the reversed twin with compatible walls of a given orientation. Contains all trivial and non-trivial symmetry operations of the domain twin (see the next section).

Classification: symbol that specifies the type of domain twin and the wall. Five types of twins and domain walls are given in Table 3.4.4.3. The letter S denotes a symmetric domain twin (wall) in which the structures in two half-spaces are related by a symmetry operation of the twin, A denotes an asymmetric twin where there is no such relation. The letters R (reversible) and I (irreversible) signify whether a twin and reversed twin are, or are not, crystallographically equivalent in K_{1j}.

Example 3.4.3.7. The rhombohedral phase of perovskite crystals. Examples include PZN-PT and PMN-PT solid solutions (see *e.g.* Erhart & Cao, 2001) and $BaTiO_3$ below 183 K. The phase transition has symmetry descent $m\bar{3}m \supset 3m$.

In Table 3.4.2.7 we find that there are eight domain states and eight ferroelectric domain states. In this fully ferroelectric phase, domain states can be specified by unit vectors representing the direction of spontaneous polarization. We choose $\mathbf{S}_1 \equiv [111]$ with corresponding symmetry group $F_1 = 3_p m_{z\bar{y}}$.

From eight domain states one can form $7 \times 8 = 56$ domain pairs. These pairs can be divided into classes of equivalent pairs which are specified by different twinning groups. In column K_{1j} of Table 3.4.2.7 we find three twinning groups:

(i) The first twin law $\bar{3}_p^{\star} m_{x\bar{y}}$ characterizes a non-ferroelastic pair $(\mathrm{Fam}\bar{3}_p^{\star} m_{x\bar{y}} = \mathrm{Fam}3_p^{\star} m_{x\bar{y}})$ with inversion $\bar{1}$ as a twinning operation of this pair. A representative domain pair is $(\mathbf{S}_1, g_{12}\mathbf{S}_1 = \mathbf{S}_2) = ([111], [1\bar{1}\bar{1}])$, domain pairs consist of two domain states with antiparallel spontaneous polarization ('180° pairs'). Domain walls of low energy are not charged, *i.e.* they are parallel with the spontaneous polarization.

(ii) The second twinning group $K_{13} = \bar{4}3m$ characterizes a ferroelastic domain pair $(\mathrm{Fam}\bar{4}3m = m\bar{3}m \neq \mathrm{Fam}F_1 = \bar{3}_p m_{z\bar{y}})$. In Table 3.4.3.6, we find $g_{13}^{\star} = 2_x^{\star}$, which defines the representative pair $([111], [\bar{1}\bar{1}1])$ ('109° pairs'). Orientations of compatible domain walls of this domain pair are (100) and $(011)_e$ (this wall is charged). All equivalent orientations of these compatible walls will appear if all crystallographically equivalent pairs are considered.

(iii) The third twinning group $K_{14} = m\bar{3}m$ also represents ferroelastic domain pairs with representative pair $([111], m_x^{\star}[111]) = ([111], [\bar{1}11])$ ('71° pairs') and compatible wall orientations $(100)_e$ and (011). We see that for a given crystallographic orientation both charged and non-charged domain walls exist; for a given orientation the charge specifies to which class the domain wall belongs.

These conclusions are useful in deciphering the 'domain-engineered structures' of these crystals (Yin & Cao, 2000).

3.4.3.6.5. *Ferroelastic domain pairs with no compatible domain walls, synoptic table*

Ferroelastic domain pairs for which condition (3.4.3.54) for the existence of coherent domain walls is violated are listed in Table 3.4.3.7. All these pairs are non-transposable pairs. It is expected that domain walls between ferroelastic domain states would be stressed and would contain dislocations. Dudnik & Shuvalov (1989) have shown that in thin samples, where elastic stresses are reduced, 'almost coherent' ferroelastic domain walls may exist.

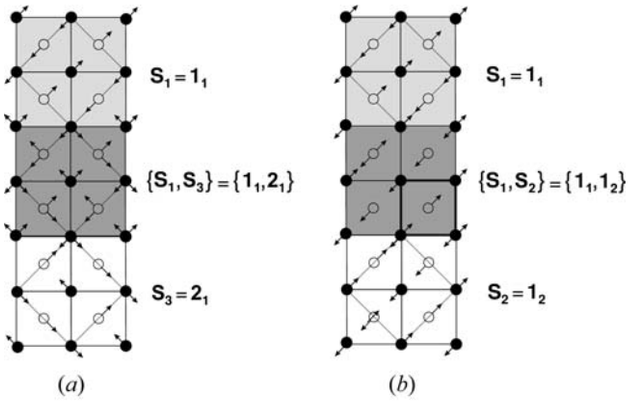

Fig. 3.4.3.10. Domain pairs in calomel. Single-domain states in the parent clamping approximation are those from Fig. 3.4.2.5. The first domain state of a domain pair is shown shaded in grey ('black'), the second domain state is colourless ('white'), and the domain pair of two interpenetrating domain states is shown shaded in dark grey. (*a*) Ferroelastic domain pair $(\mathsf{S}_1, \mathsf{S}_3)$ in the parent clamping approximation. This is a partially transposable domain pair. (*b*) Translational domain pair $(\mathsf{S}_1, \mathsf{S}_2)$. This is a completely transposable domain pair.

Example 3.4.3.8. Ferroelastic crystal of langbeinite. Langbeinite $K_2Mg_2(SO_4)_3$ undergoes a phase transition with symmetry descent $23 \supset 222$ that appears in Table 3.4.3.7. The ferroelastic phase has three ferroelastic domain states. Dudnik & Shuvalov (1989) found, in accord with their theoretical predictions, nearly linear 'almost coherent' domain walls accompanied by elastic stresses in crystals thinner than 0.5 mm. In thicker crystals, elastic stresses became so large that crystals were cracking and no domain walls were observed.

Similar effects were reported by the same authors for the partial ferroelastic phase of $CH_3NH_3Al(SO_4)_2{\cdot}12H_2O$ (MASD) with symmetry descent $\bar{3}m \supset mmm$, where ferroelastic domain walls were detected only in thin samples.

3.4.3.7. *Domain pairs in the microscopic description*

In the *microscopic description*, two microscopic domain states S_i and S_k with space-group symmetries $\mathcal{F}_i$ and $\mathcal{F}_k$, respectively, can form an ordered domain pair $(\mathsf{S}_i, \mathsf{S}_k)$ and an unordered domain pair $\{\mathsf{S}_i, \mathsf{S}_k\}$ in a similar way to in the continuum description, but one additional aspect has to be considered. The definition of the symmetry group $\mathcal{F}_{ik}$ of an ordered domain pair $(\mathsf{S}_i, \mathsf{S}_k)$,

$$\mathcal{F}_{ik} = \mathcal{F}_i \cap \mathcal{F}_k, \tag{3.4.3.72}$$

is meaningful only if the group $\mathcal{F}_{ik}$ is a space group with a three-dimensional translational subgroup (three-dimensional *twin lattice* in the classical description of twinning, see Section 3.3.8)

$$\mathcal{T}_{ik} = \mathcal{T}_i \cap \mathcal{T}_k, \tag{3.4.3.73}$$

where $\mathcal{T}_i$ and $\mathcal{T}_k$ are translation subgroups of $\mathcal{F}_i$ and $\mathcal{F}_k$, respectively. This condition is fulfilled if both domain states S_i and S_k have the same spontaneous strains, *i.e.* in non-ferroelastic domain pairs, but in ferroelastic domain pairs one has to suppress spontaneous deformations by applying the parent clamping approximation [see Section 3.4.2.2, equation (3.4.2.49)].

Example 3.4.3.9. Domain pairs in calomel. Calomel undergoes a non-equitranslational phase transition from a tetragonal parent phase to an orthorhombic ferroelastic phase (see Example 3.4.2.7 in Section 3.4.2.5). Four basic microscopic single-domain states are displayed in Fig. 3.4.2.5. From these states, one can form 12 non-trivial ordered single-domain pairs that can be partitioned (by means of double coset decomposition) into two orbits of domain pairs.

Representative domain pairs of these orbits are depicted in Fig. 3.4.3.10, where the first microscopic domain state S_i participating in a domain pair is displayed in the upper cell (light grey) and the second domain state S_j, $j = 2, 3$, in the lower white cell. The overlapping structure in the middle (dark grey) is a geometrical representation of the domain pair $\{\mathsf{S}_1, \mathsf{S}_j\}$.

The domain pair $\{\mathsf{S}_1, \mathsf{S}_3\}$, depicted in Fig. 3.4.3.10(*a*), is a ferroelastic domain pair in the parent clamping approximation. Then two overlapping structures of the domain pair have a common three-dimensional lattice with a common unit cell (the dotted square), which is the same as the unit cells of domain states S_1 and S_3.

Domain pair $\{\mathsf{S}_1, \mathsf{S}_2\}$, shown in Fig. 3.4.3.10(*b*), is a translational (antiphase) domain pair in which domain states S_1 and S_2 differ only in location but not in orientation. The unit cell (heavily outlined small square) of the domain pair $\{\mathsf{S}_1, \mathsf{S}_2\}$ is identical with the unit cell of the tetragonal parent phase (*cf.* Fig. 3.4.2.5).

The two arrows attached to the circles in the domain pairs represent exaggerated displacements within the wall.

Domain pairs represent an intermediate step in analyzing microscopic structures of domain walls, as we shall see in Section 3.4.4.

3.4.4. Domain twins and domain walls

3.4.4.1. *Formal description of simple domain twins and planar domain walls of zero thickness*

In this section, we examine crystallographic properties of planar compatible domain walls and simple domain twins. The symmetry of these objects is described by layer groups. Since this concept is not yet common in crystallography, we briefly explain its meaning in Section 3.4.4.2. The exposition is performed in the continuum description, but most of the results apply with slight generalizations to the microscopic treatment that is illustrated with an example in Section 3.4.4.7.

We shall consider a *simple domain twin* $\mathbf{T}_{12}$ that consists of two domains $\mathbf{D}_1$ and $\mathbf{D}_2$ which meet along a planar domain wall $\mathbf{W}_{12}$ of zero thickness. Let us denote by p a *plane of the domain wall*, in brief *wall plane* of $\mathbf{W}_{12}$. This plane is specified by Miller indices (hkl), or by a normal $\mathbf{n}$ to the plane which also defines the sidedness (plus and minus side) of the plane p. By *orientation of the plane p* we shall understand a specification which can, but may not, include the sidedness of p. If both the orientation and the sidedness are given, then the plane p divides the space into two half-spaces. Using the bra–ket symbols, mentioned in Section 3.4.3.6, we shall denote by $(\,|$ the half-space on the negative side of p and by $|\,)$ the half-space on the positive side of p.

A *simple twin* consists of two (theoretically semi-infinite) domains $\mathbf{D}_1$ and $\mathbf{D}_2$ with domain states $\mathbf{S}_1$ and $\mathbf{S}_2$, respectively, that join along a planar domain wall the orientation of which is specified by the wall plane p with normal $\mathbf{n}$. A symbol $(\mathbf{S}_1|\mathbf{n}|\mathbf{S}_2)$ specifies the domain twin unequivocally: domain $(\mathbf{S}_1|$, with domain region $(\,|$ filled with domain state $\mathbf{S}_1$, is on the negative side of p and domain $|\,\mathbf{S}_2)$ is on the positive side of p (see Fig. 3.4.4.1*a*).

If we were to choose the normal of opposite direction, *i.e.* $-\mathbf{n}$, the same twin would have the symbol $(\mathbf{S}_2|-\mathbf{n}|\mathbf{S}_1)$ (see Fig. 3.4.4.1*a*). Since these two symbols signify the same twin, we have the identity

$$(\mathbf{S}_1|\mathbf{n}|\mathbf{S}_2) \equiv (\mathbf{S}_2|-\mathbf{n}|\mathbf{S}_1). \tag{3.4.4.1}$$

Thus, if we invert the normal $\mathbf{n}$ and simultaneously exchange domain states $\mathbf{S}_1$ and $\mathbf{S}_2$ in the twin symbol, we obtain an identical twin (see Fig. 3.4.4.1*a*). This identity expresses the fact that the